

## CHAPTER IV

### RESULT AND DISCUSSION

#### Tamarind seed coat extraction

##### Characteristics of tamarind seed coat extract

The crude extract from tamarind seed coat after liquid extraction and evaporation process was light-brown powder (Figure 18). The percent yield of the extract obtained was  $25.4 \pm 1.2\%$  w/w. The extract was water-soluble and dissolved easily to solution form. This powder was kept in a tight container at 4°C for further studies.



**Figure 18** The appearance of tamarind seed coat extract

##### Quantification of total phenol in the extract

Sudjaroen, et al. (2005) reported the main components of tamarind seed coat extract, which were catechin, epicatechin and procyanidin. To quantify the total amount of major antioxidant in the extract, the assay of total phenol in the extract was performed.

As determined by Folin-Ciocalteu assay, the amount of the phenolic compounds contained in the extract was  $85.6 \pm 0.9$  mg catechin equivalents per gram extract (Appendix B). The obtained results well coincide with those obtained from previous study (Soong and Barlow, 2004). As mentioned earlier, tannin is one of component in tamarind seed coat extract. Since the characteristic reaction of tannins are their ability to precipitate cell protein, this was not considered to use in cell culture *in vitro* study. Therefore, tannin was removed by Sephadex LH20 column before being total phenol quantification assay.

#### Free radical scavenging activity of the extract

The antioxidant potential is inversely proportional to  $EC_{50}$  value, which was calculated from the non-linear regression of the percentage of remaining DPPH against the extracts/standard concentrations (Appendix C). The lower  $EC_{50}$  value indicates the higher antioxidant activity. According to the obtained results (Figure 19), the  $EC_{50}$  of tamarind seed coat extract was 12.92  $\mu\text{g/ml}$ . While the  $EC_{50}$  of L-ascobic acid (vitamin C) and tocopherol (vitamin E) were 22.86 and 29.34  $\mu\text{g/ml}$  respectively. This result coincides to previous study (Pumthong, 1999) that indicated the stronger antioxidant activity of tamarind seed coat extract than the well-known antioxidant compounds.

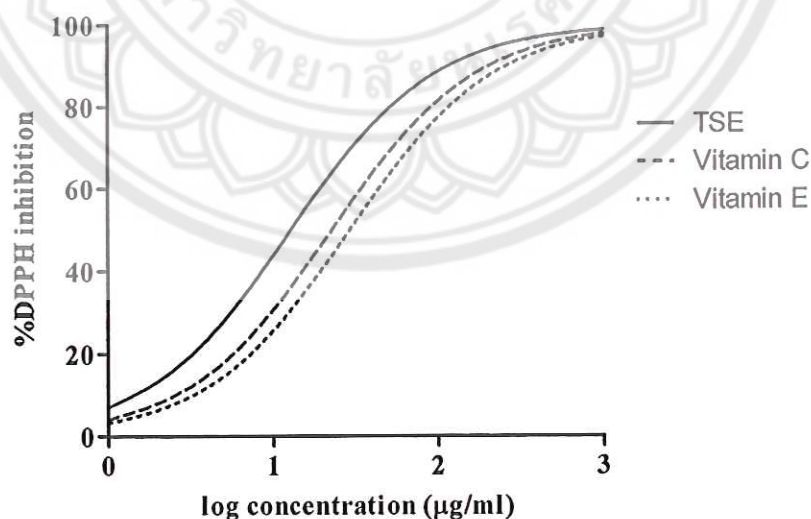


**Figure 19** Free radical scavenging activity of tamarind seed coat extract (TSE) from DPPH assay. Each bar represents mean  $\pm$  SD of triplicate study

### Cytotoxicity of tamarind seed coat extract

To determine the skin cytotoxicity of tamarind seed coat extract, preliminary screening of skin cell viability against the extract concentration was studied. HaCaT (normal human keratinocyte) represented the skin simulation. The 97-91% viability of HaCaT after treated for 24 h with 50–200  $\mu\text{g/ml}$  extract was not significantly different ( $p < 0.05$ ) from control (untreated cell) (Figure 20).

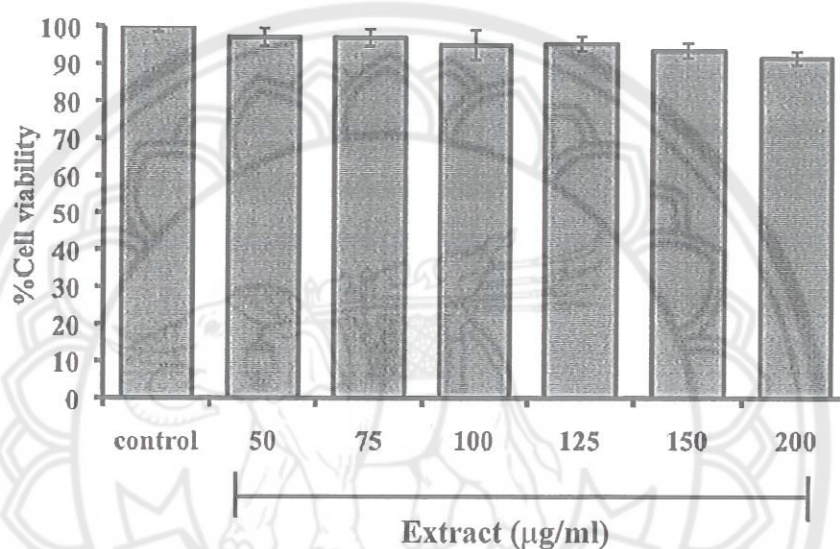


**Figure 20** HaCaT cell viability after treated with tamarind seed coat extract at concentrations in range of 50-200  $\mu\text{g/ml}$  for 24 h. Each bar represents mean  $\pm$  SD of triplicate study

Moreover, even at highest concentration tested (200  $\mu\text{g/ml}$ ), HaCaT was not changed in morphology as shown in Figure 21. It could imply that the efficacious concentrations of tamarind seed coat extract are non-toxic to skin cell *in vitro*. This study led to proper concentration used of tamarind seed coat extract in other studies.



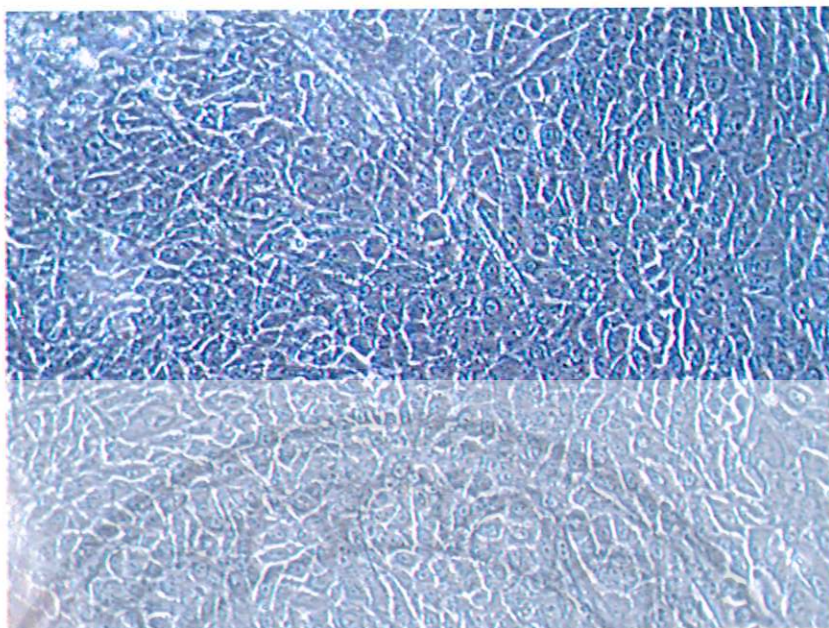


**Figure 21 Morphology of HaCaT after treated with 200 µg/ml extract at magnification of 20X**

#### **The lightening efficacy of tamarind seed coat extract**

##### **Effects of extract on melanogenesis in B16-F1 (mouse melanoma cell)**

The potential of any substance that can improve skin pigmentation is reducing total melanin content in the skin. To prove the potential of tamarind seed coat extract in reducing melanin content, mouse melanoma cell line (B16-F1) is a proper model because its released melanin can clearly observed spectrophotometrically. The melanogenesis activity of B16-F1 cells was investigated by determining content of the melanin produced by cells (Appendix D). The extract showed the dose-dependent inhibition and protection of melanin production of B16-F1 cells stimulated by  $\alpha$ -MSH, as shown in Figure 22. In the presence of extract (50–200 µg/ml), there was a concentration dependent reduction in melanin production, which depended on the protocol used. The results show that extract dose-dependently caused some reduction melanin content of B16-F1 melanoma cells pre-stimulated by  $\alpha$ -MSH.

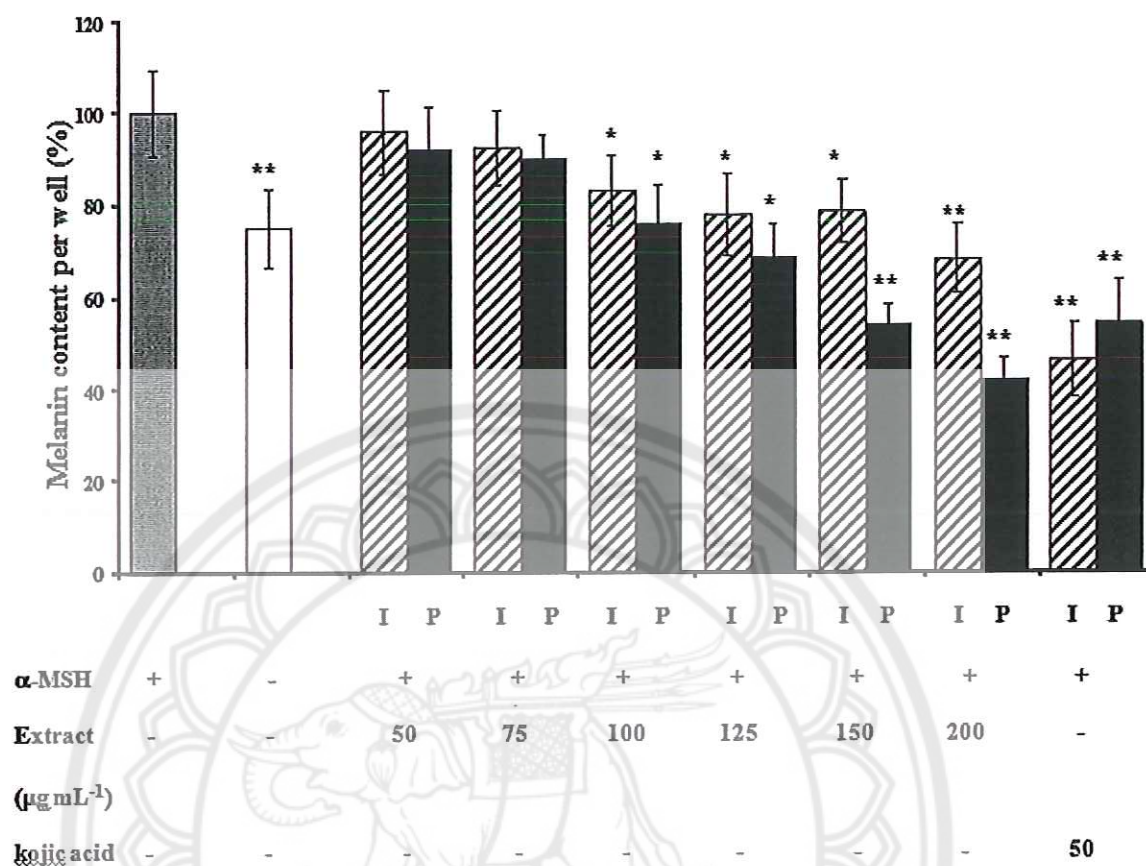


**Figure 22** Tamarind seed coat extract reduced melanin production. B16-F1 melanoma cells were treated with the extract at concentrations in range of 50-200  $\mu\text{g/ml}$  after (inhibition, I) or before (protection, P) being stimulated with  $\alpha$ -MSH. Each bar represents mean  $\pm$  SD of triplicate study. \* $P < 0.05$  and \*\* $P < 0.01$  denote significant differences when compared to control (Student's  $t$ -test)

Interestingly, as compared to the  $\alpha$ -MSH-stimulated cells without extract treatment, the percentage of melanin reduction was about 20-32% in the cells treated with the extract at high concentration (150-200  $\mu\text{g/ml}$ ) after being stimulated with  $\alpha$ -MSH (inhibition condition) whereas the melanin reduction was about 42-59% in the cells treated with the extract at the similar concentrations before being stimulated with  $\alpha$ -MSH (prevention condition). For kojic acid (50  $\mu\text{g/ml}$ ), which was used as a reference inhibitor, the decrease in melanin content was observed at about 50% in both inhibition and protection conditions. Our findings indicate that the protection effect of



the extract was greater than the inhibition effect. This implies that the extract competes with both the downstream activation of  $\alpha$ -MSH and the upstream control of melanogenesis perhaps including  $\alpha$ -MSH-MC1R binding.

Furthermore, the extract was not significantly affected on cell viability within the range of tested concentrations, as shown in Figure 23. This indicated that the reduction of melanin production was not due to cell death.

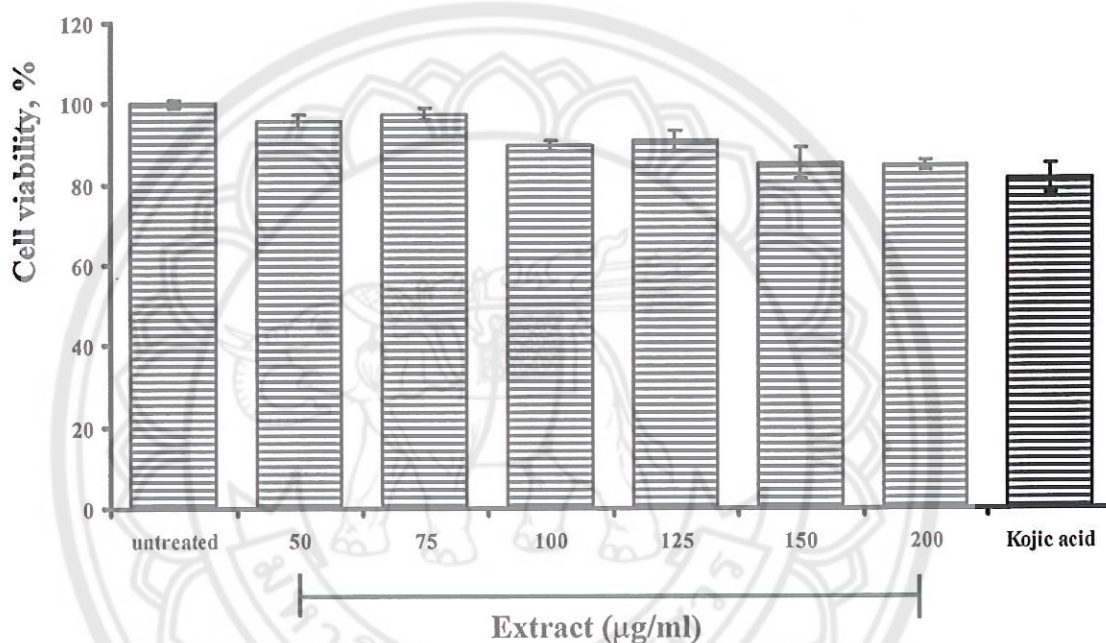


**Figure 23** The viability of B16-F1 mouse melanoma cells treated with tamarind seed coat extract at concentrations in range of 50-200  $\mu$ g/ml for 24 h. Each bar represents mean  $\pm$  SD of triplicate study

Interestingly, all concentrations tested of the extract did not change the morphology of B16-F1 while 50  $\mu$ g/ml kojic acid did, as shown in Figure 24. This indicated that, even both compounds possess strong melanogenesis activities, tamarind seed coat extract seem to be less toxic than kojic acid.



**Figure 24** Morphology of B16-F1 mouse melanoma cells after treated with 200  $\mu\text{g/ml}$  tamarind seed coat extract (A) and 50  $\mu\text{g/ml}$  kojic acid (B) at magnification of 40X

## **Melanogenic activity of the extract in human primary cells**

### **1. Cultivation of keratinocyte-melanocyte co-culture**

The isolation of keratinocyte-melanocyte co-culture from skin tissue in different area (foreskin, eyelid and abdominal) was developed. The morphology of cells was shown in Figure 25. As expected, the shapes of keratinocyte-melanocyte from different area epidermis were looked alike. While melanocytes surrounded by keratinocyte were evenly distributed over the surface, melanocyte tended to crawl over keratinocyte. Fresh culture formed a complete monolayer after 1-2 weeks. By this time, the content of melanocyte was 4-7% of the total cell count. However, keratinocyte-melanocyte co-culture from foreskin seems to be stronger than the others, observed by the highest viability of melanocyte after isolation and cultivation. In this reason, keratinocytes and melanocytes isolated from foreskin tissues coming from humans' aged  $\leq 3$  years without any melanogenesis stimulator was used in order to mimic the melano-epidermic activity.



**Figure 25 Morphology of human keratinocyte-melanocyte co-culture at magnification of 40X**



## 2. Cytotoxicity of tamarind seed coat extract on keratinocyte-melanocyte co-culture

To ensure that melanogenesis activity of the extract occurred from normal cell function not from cell death or reduced cell replication. Viability following treatment was determined by counting the number of trypan blue positive cells in each well under x100 microscope. The results showed that no significantly different in morphology and number of cell between tamarind seed coat treated group and untreated group (Figure 26)

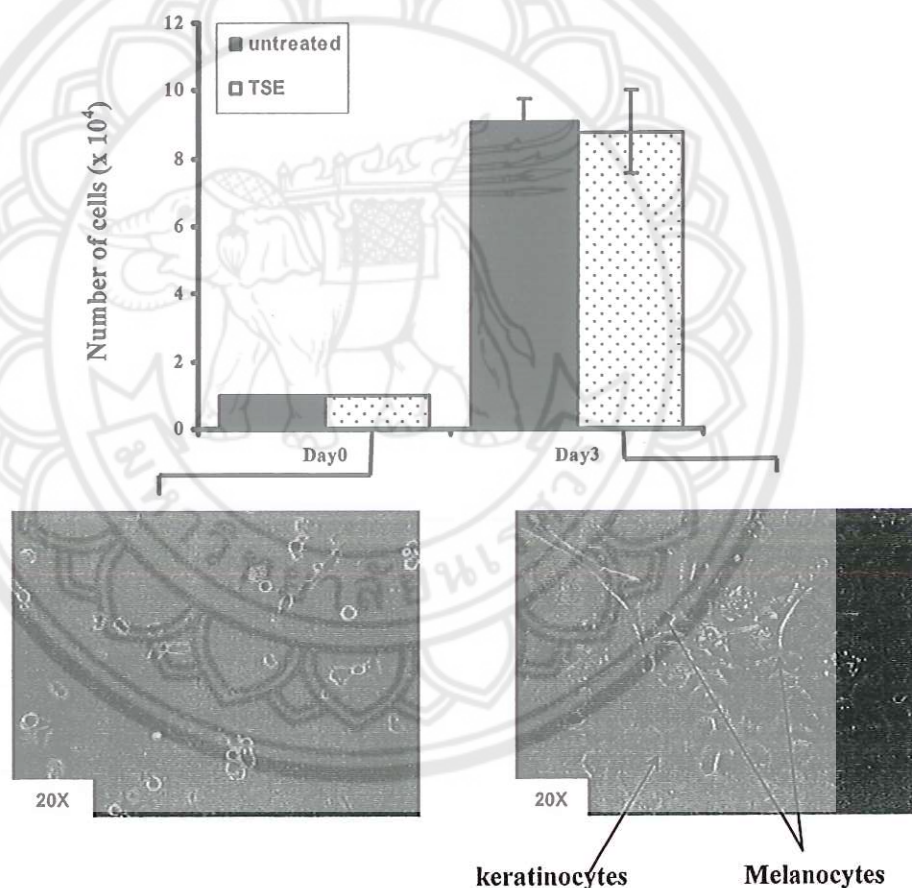


**Figure 26** The viability and morphology of human keratinocyte-melanocyte co-culture treated with 200  $\mu\text{g/ml}$  (open bar) of tamarind seed coat extract and untreated (control) (filled bar) at day 0 and day 3. Each bar represents mean  $\pm$  SD of study from three batches of keratinocyte-melanocyte co-culture cells.

### 3. Effect of the extract on tyrosinase activity

Other plant extracts and their bioactive constituents have been explored previously for tyrosinase inhibitory activity (Yoon, et al., 2011; Momtaz, et al., 2008). Polyphenols, such as epicatechin, epigallocatechin, and epicatechin-3-gallate, isolated from plants proved to be effective inhibitors of tyrosinase. Thus polyphenols in our extract may also inhibit tyrosinase and/or inhibit L-DOPA auto-oxidation. Here, keratinocyte and melanocyte were co-cultured without any melanogenesis stimulator thus mimicing in vivo melano-epidermic activity using dopachrome formation from L-DOPA. From the results obtained,  $IC_{50}$  value as determined by plotting between the log concentration of the test agent and percent inhibition of dopachrome formation was  $152.1 \pm 10.2 \mu\text{g/ml}$  for the extract whereas that of the kojic acid was  $33.3 \pm 2.5 \mu\text{g mL}^{-1}$  (Figure 27). The extract was clearly less potent compared to kojic acid although the maximum effects were similar (94.7% for extract and 96.6% kojic acid) (Appendix E).

Moreover, the morphology of both the keratinocytes and melanocytes appeared to be unaffected by the extract (200  $\mu\text{g/ml}$ ). Furthermore, the cell counts were unchanged in the culture conditions suggesting that the reduced tyrosinase activity did not result from cell death or reduced cell replication. This might include chelation of copper ion within the tyrosinase or the phenolic hydroxyls binding to the enzyme causing stearic hindrance (Yoon, et al., 2011). For kojic acid treated group, we found that kojic acid at high concentrations ( $\geq 100 \mu\text{g/ml}$ ) caused changes in cell morphology, and such changes might influence the tyrosinase amount and activity.



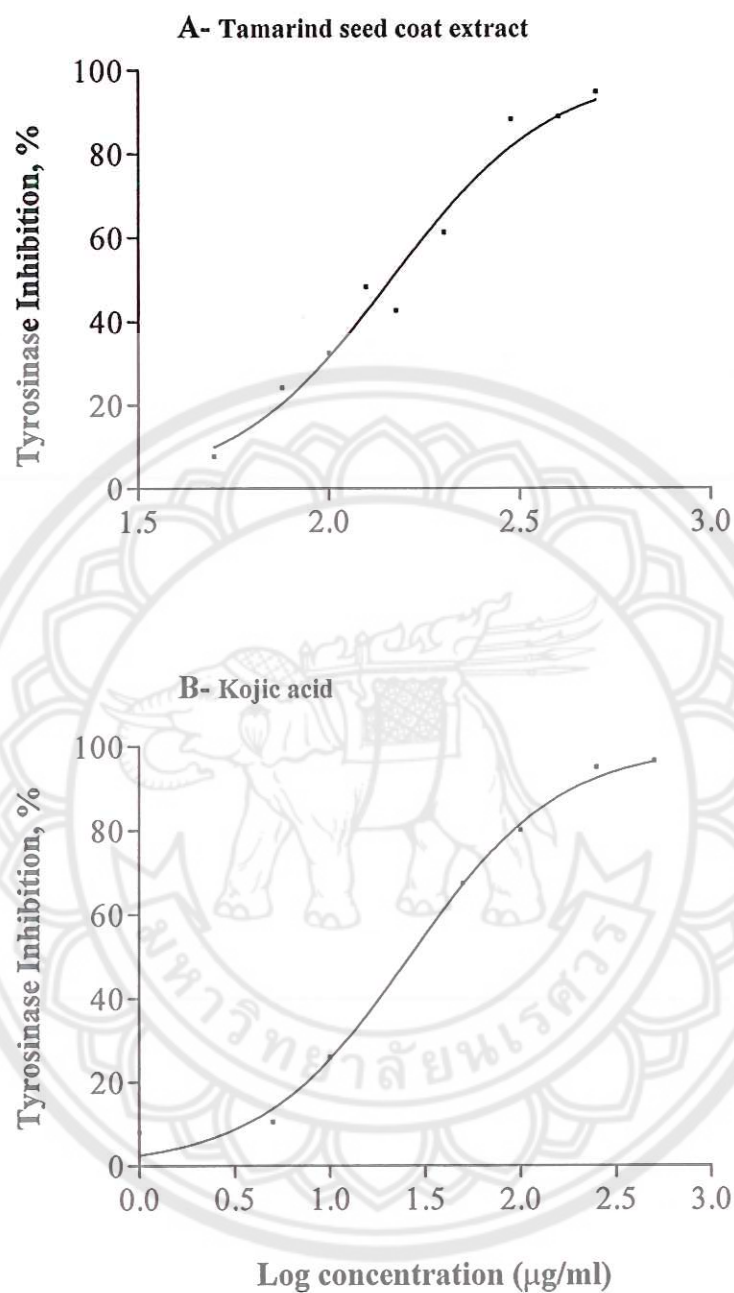


**Figure 27** Percent inhibition of tyrosinase activity by tamarind seed coat extract (A) or kojic acid (B). The study was performed in three batches of keratinocyte-melanocyte co-culture cells isolated from one-skin tissues.

#### 4. Intracellular calcium and PAR-2 activity

The melanogenesis steps in skin include melanin synthesis and transportation of melanin from melanocyte to keratinocyte. In this reason, the present study was designed to examine the possibility that tamarind seed coat extract could also affect pigmentation by inhibiting the PAR-2 activity. PAR-2 is expressed mainly in keratinocyte and increased activity of PAR-2 in keratinocytes causes increasing uptake and distribution of melanosomes by keratinocytes in the epidermis. In this reason, keratinocyte-melanocyte co-culture model was used to mimic the physiological situation happening when melanocytes and keratinocytes co-operate for the transfer of melanins. The natural PAR-2 activator (trypsin, TRP) was used to determine the receptor activity and also consistency of keratinocyte-melanocyte distribution of each batch of isolated co-culture. The results from fluorescence values of staining calcium expressed as a percentage are shown in Figure 28, Appendix F.

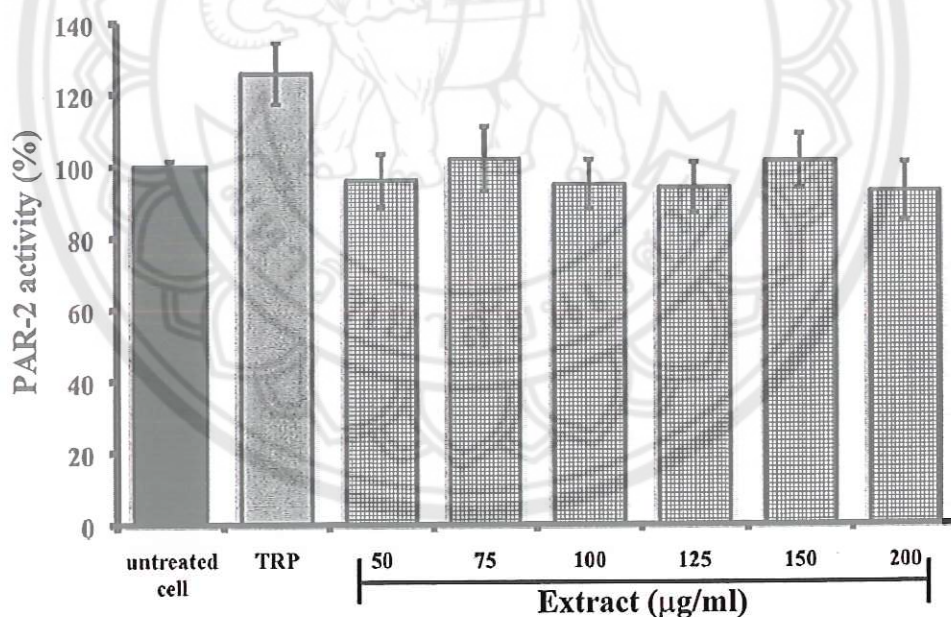


**Figure 28** Tamarind seed coat extract and intracellular calcium related to PAR-2 activity. Trypsin (TRP, 10 µM) was used as a PAR-2 activator. Each bar represents mean  $\pm$  SD of three batches of keratinocyte-melanocyte co-culture cells



As similar to another study (Paine, et al., 2001), the activation by TRP significantly promoted PAR-2 activity ( $p < 0.01$ ) as compared to the untreated group. Tamarind seed coat extract at any concentration used did not alter PAR-2 activity. Although the direct inhibitory effect of the extract on PAR-2 did not exhibit, it cannot not be concluded that the extract does not affect melanosome transfer. Recent studies indicate that the skin depigmentation of soymilk and the soybean-derived serine protease inhibitors is not directly involved with receptor inhibition but correlates with blocking action of trypsin, resulting in a decreased transfer of melanosome (Seiberg, et al., 2000b; Paine, et al., 2001). Therefore, further study should be performed to determine depigmentation by extract via inhibition of the PAR-2 pathway.

#### **Anti-aging efficacy of tamarind seed coat extract**

##### **Development of skin fibroblast from explant technique**

Normally, the biomolecular model that widely used for skin aging evaluation was fibroblast cell culture (Varani, et al., 2006; Morisaki, et al., 2010; Rock, et al., 2011). Here, fibroblast was isolated from excess skin surgery in different area such as abdominal, eyelid and breast. Mostly, the donors are women both Caucasians and Asian aged from 29-65 years old.

After explant the skin tissue on disk, the pattern of fibroblast migration was the same in every skin type (Figure 29). The differentiation was time period of migration. In young (age not more than 35) and fresh skin tissue, fibroblast began migrated from explant tissue within 5-7 days of incubation. The period was extending for 15-30 days in old or wrinkle skin tissue (wrinkled skin area). With elongate and spindled cell body, fibroblasts when crowded often locally align in parallel clusters.

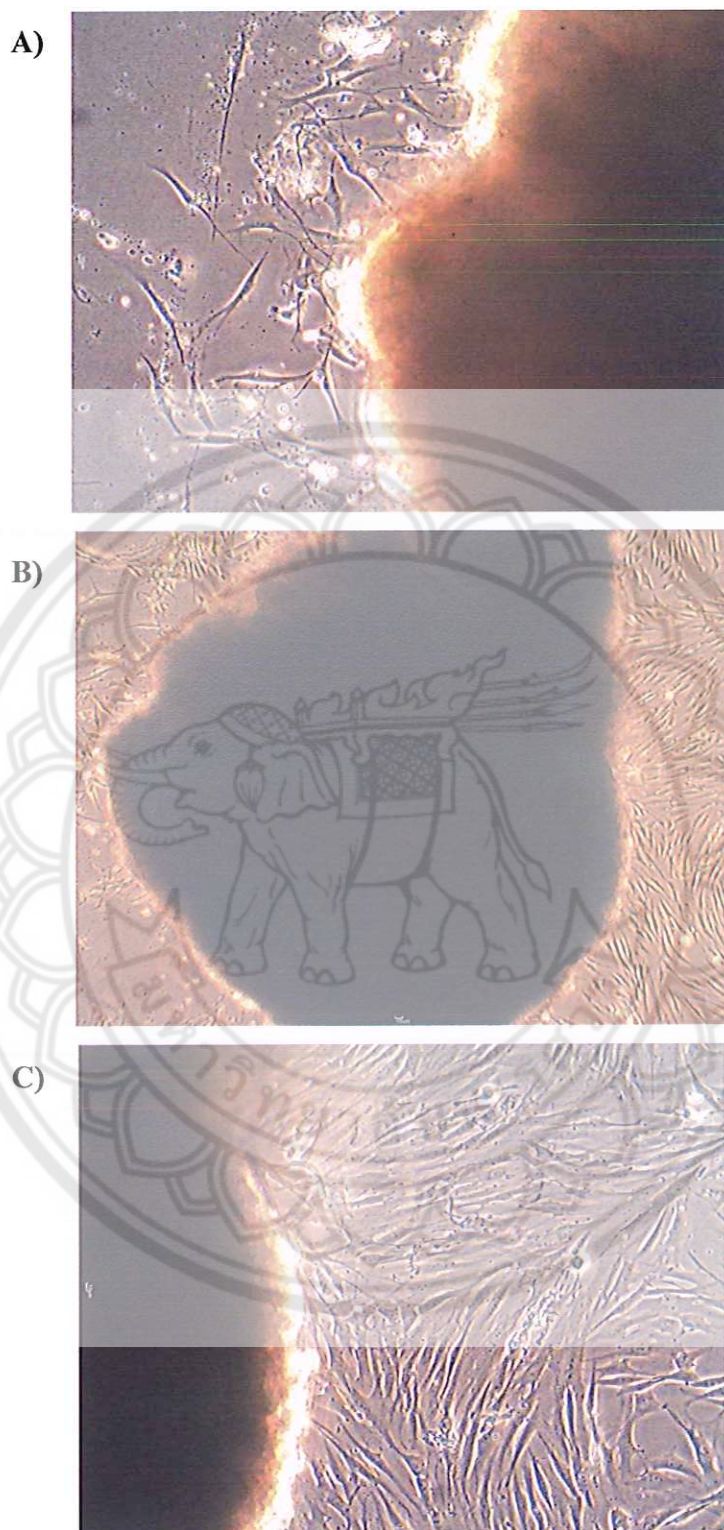


**Figure 29** Fibroblast cells migrated from explant tissue from abdominal of woman aged 35 years old at day 7 (A), day 10 (B) and confluent at day 20 (C) visualized under 10X - 20X microscope.



### Prevention of H<sub>2</sub>O<sub>2</sub> induced fibroblast damage

Hydrogen peroxide (H<sub>2</sub>O<sub>2</sub>) is an active oxygen species that can diffuse freely into cells and is relatively more stable compared with superoxide anions or hydroxyl radicals (Davies, et al., 1999). Hydrogen peroxide is first converted to a hydroxyl radical, which is a very strong oxidant before being converted to water. Using H<sub>2</sub>O<sub>2</sub> as a source of oxidant, we studied the cellular damage to oxidative stress in primary human skin fibroblasts. Our data showed that doses of H<sub>2</sub>O<sub>2</sub> (100-1000  $\mu$ M/ml) induce rapid cell death (62-92%), Figure 30 (Appendix H).

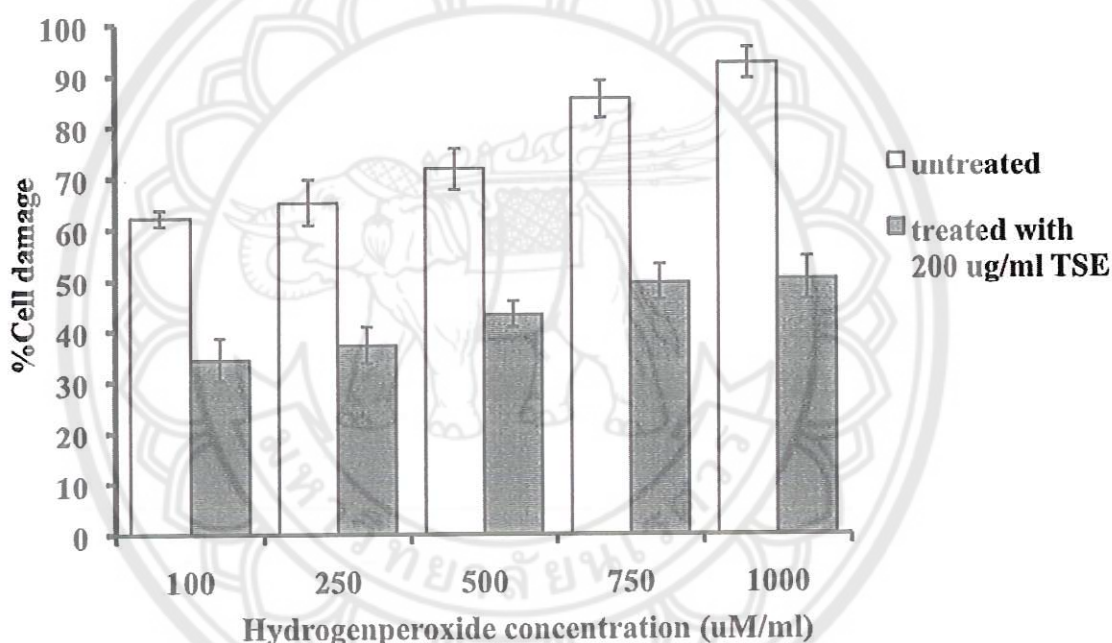


**Figure 30** Percentage of cell damage in H<sub>2</sub>O<sub>2</sub>-induced fibroblast; TSE = group of cells treated with 200 ug/ml extract. Each bar represents mean  $\pm$  SD of triplicate study.

As expected, protective effect of tamarind seed coat extract expressed as a percentage of the cell viability from 34-45%. The mechanism of cellular protection might occur from free radical scavenging activity of tamarind seed coat extract. Polyphenols in the extract possess ideal structural chemistry for free radical scavenging activity. Antioxidative properties of polyphenols arise from their high reactivity as hydrogen or electron donors, and from the ability of the polyphenol

derived radical to stabilize and delocalize the unpaired electron (Rice-Evans, et al., 1997). Another mechanism underlying the antioxidative properties of the extract is the ability of flavonoids to alter peroxidation kinetics by modification of the lipid packing order and to decrease fluidity of the membranes (Arora, et al., 2000). These changes could sterically hinder diffusion of free radicals and restrict peroxidative reactions. These actions could protect cell from membrane lipid peroxidation and apoptosis. Our preliminary results suggest that the cellular protective properties of tamarind seed coat extract against oxidative stress might improve the skin aging.

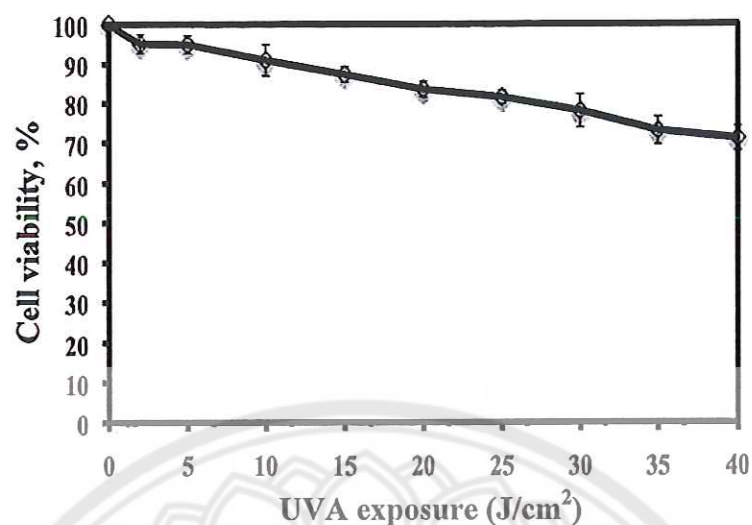
#### **Effect of tamarind seed coat extract to improve UVA-induced aged fibroblast**

An understanding of the cellular responses to oxidative stress will provide useful insights into the mechanisms of aging and transformation.

##### **1. Tamarind seed coat inhibits UVA-induced fibroblast cell death**

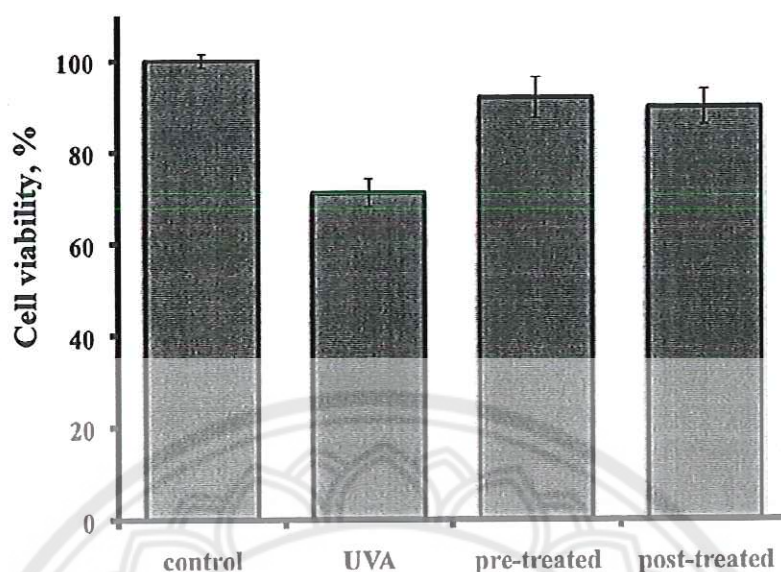
To confirm the cytotoxic effect of UVA irradiation, we exposed cultured fibroblast cells to increasing doses of UVA radiation (5 - 40 J/cm<sup>2</sup>). Cell viability was determined at 24 h after UVA irradiation. As expected, fibroblast cells death occurred after UVA exposure in our system. The decrease of cell viability was UVA-dose-dependent, resulting in 96 - 71% of remaining survivals at 5 - 40 J/cm<sup>2</sup>, respectively (Figure 31). Since 40 J/cm<sup>2</sup> of UVA irradiation caused significantly different in cell viability (71%), this dosage was used in the following studies on the protective effect on UVA-induced cytotoxicity. However, the results of cell viability after UVA irradiated depended on the variation including cell passages and sources of fibroblast (young and old skin). Young fibroblasts with freshly passage (not exceed 6) tend to be more potent than old fibroblast.





**Figure 31** The viability of fibroblast cells with UVA-irradiation in range of 5-40 J/cm<sup>2</sup>. Each bar represents mean  $\pm$  SD of triplicate study

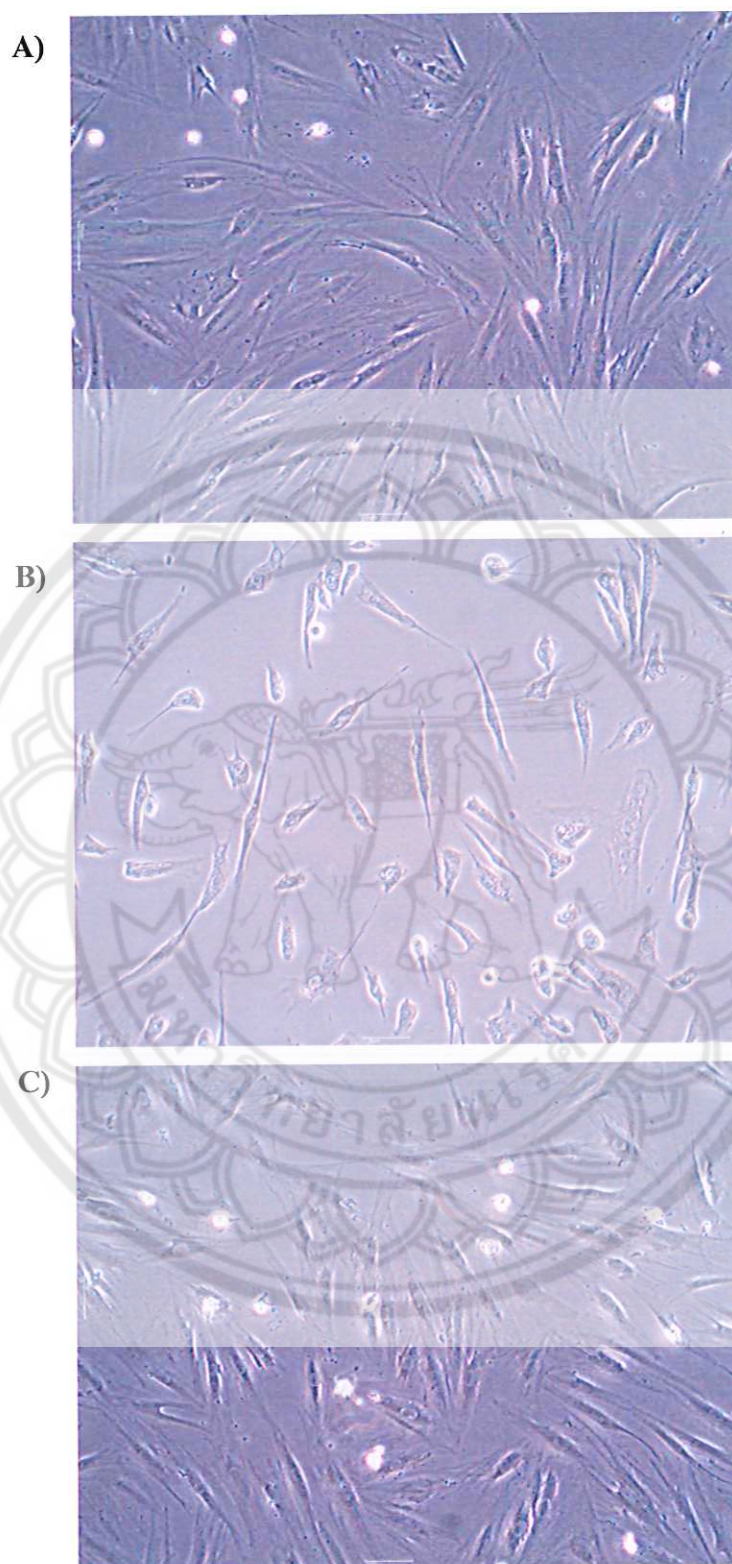
To determine the protective effects of tamarind seed coat extract on UVA-induced fibroblast damage, we performed a cell viability assay. The XTT assay showed that cell viability of fibroblast was decreased after UVA exposure. However, the decrease was reversed by the treatment of tamarind seed coat (pre and post treated with 200  $\mu$ g/ml) as showed in Figure 32. Approximately 85% and 84% of cells were viable upon pre-treated and post-treated UVA exposure, respectively. The different in cell survival rate under UVA with and without the extract was significant ( $p < 0.05$ ). These observations indicated that tamarind seed coat extract is effective in the prevention of UVA-induced fibroblast damage.



**Figure 32** The viability of UVA-induced fibroblast cells treated with 200  $\mu\text{g/ml}$  tamarind seed coat extract. Each bar represents mean  $\pm$  SD of triplicate study

Moreover, the visualization of fibroblast morphology was performed to investigate the UVA-induced cell damage. Figure 33 showed the morphology of UVA-induced fibroblast untreated and treated with 200  $\mu\text{g/ml}$  extract under 20X microscope. The changed in morphology of fibroblasts appeared when induced with UVA compared to control cell (Figure 33A-B), damage cell became irregular round shape. Beside, fibroblasts still retained the typical spindle shaped after treatment with the extract (Figure 33C).

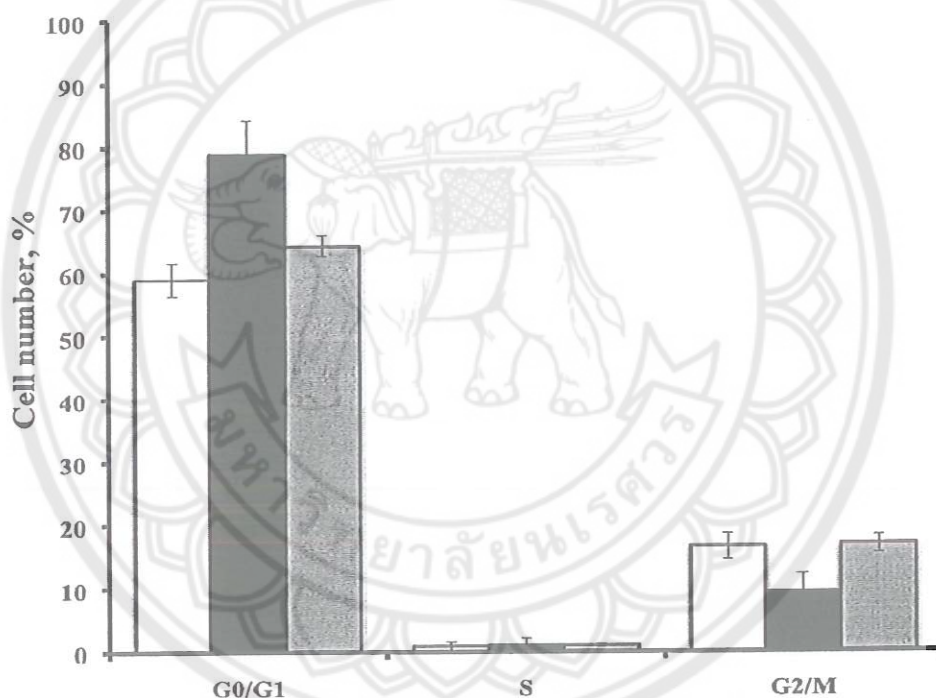




**Figure 33 Morphology of fibroblast under 20X microscope; normal fibroblast (A), UVA-induced fibroblast (B) and UVA-induced fibroblast treated with 200 µg/ml extract (C)**

## 2. Cell cycle analysis

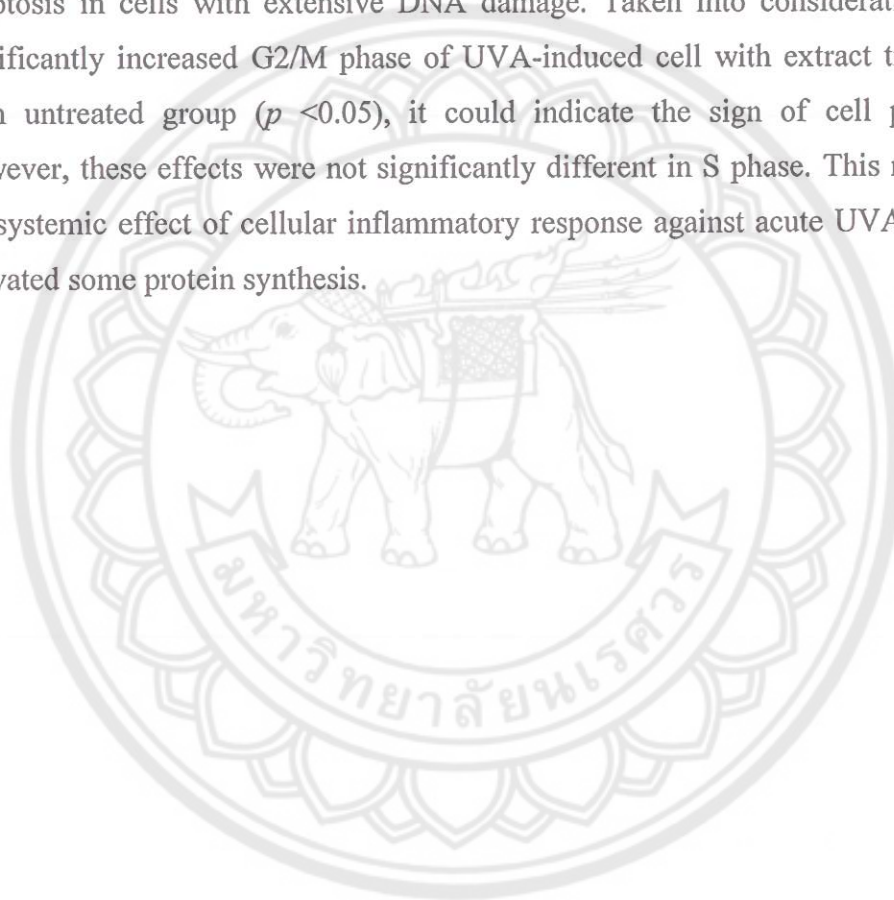
Cell cycle regulation plays an important role in maintaining the genetic integrity of the cell. UV treatment of skin fibroblast cells resulted in cell cycle alterations, especially in the suppression of G0/G1 phase progression and induction of S and G2/M phase arrest. In this study, a cell cycle of the UVA-induced fibroblasts treated with extract was conducted by flow cytometry. The cell cycle stages in control cells, UVA untreated cell and UVA treated cells with 200  $\mu\text{g/ml}$  extract are summarized in Figure 34 and histograms of the flow cytometric data are shown in Figure 35 and Appendix H.



**Figure 34** Cell cycle of fibroblast in normal condition (open bar), UVA-irradiated cells (black filled bar) and UVA-irradiated cells treated with 200  $\mu\text{g/ml}$  (gray filled bar) of tamarind seed coat extract after 72h cultivation. Each bar represents mean  $\pm$  SD of triplicate study.



The results obtained shows that UVA-induced fibroblast increase G0/G1 phase to 78% from normal condition (59%), and decreased G2/M phase (9%) from 16%. A prolonged G1 phase of the cell cycle due to the accumulation of the activated p53 protein is a characteristic of UVA damaged cells (Karin, et al., 2002). Interestingly, treatment of UV-irradiated cells with tamarind seed coat extract significantly restored the suppressed G0/G1 progression (64%), this allows cells enough time to repair DNA damage before its replication in the S phase or it induces apoptosis in cells with extensive DNA damage. Taken into consideration with the significantly increased G2/M phase of UVA-induced cell with extract treated group from untreated group ( $p < 0.05$ ), it could indicate the sign of cell proliferation. However, these effects were not significantly different in S phase. This might due to the systemic effect of cellular inflammatory response against acute UVA damage by activated some protein synthesis.



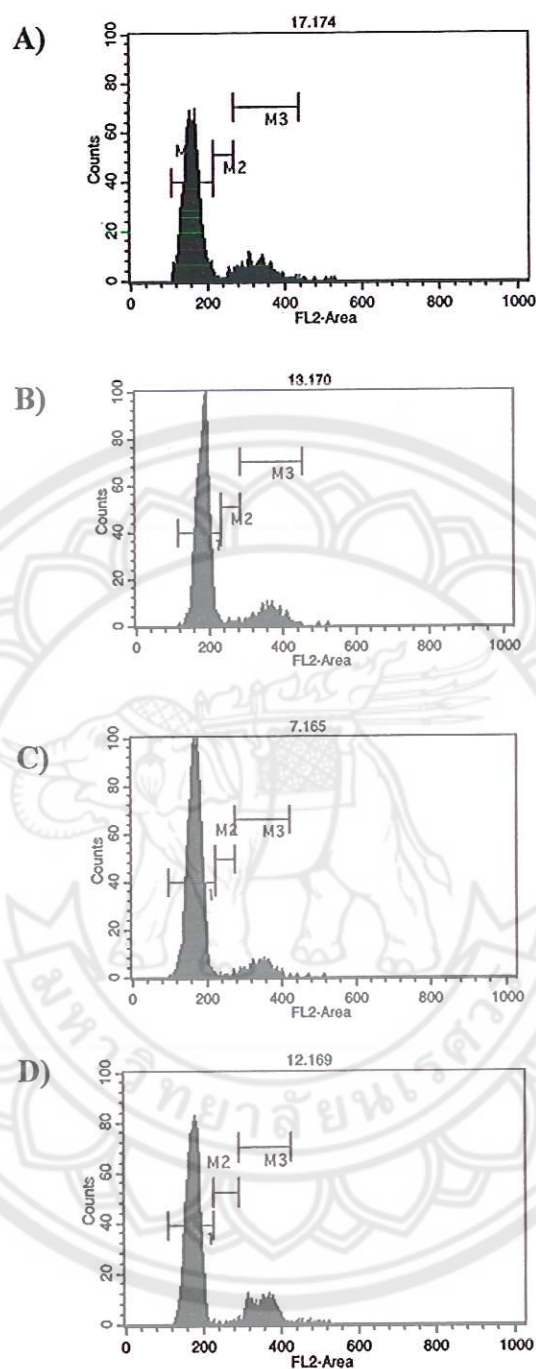


**Figure 35** Histogram of flow cytometric data of young fibroblast in normal condition (A), aged skin (B), UVA-irradiated cells (C) and UVA-irradiated cells treated with 200 µg/ml (D) of tamarind seed coat extract after 72h cultivation



### 3. Improvement of intracellular glutathione deficiency

The intracellular glutathione concentration is the final result of a balance between GSH generation (via synthesis and recycling from GSSG by glutathione reductase) and the combined rate of GSH consumption by ROS and excretion of the resulting GSSG. Under normal conditions 95% of the intracellular glutathione is present in its reduced GSH form. The oxidized GSSG form can either be recycled to GSH or removed from the intracellular total GSH content or the GSH/GSSG balance.

In this study, the total glutathione level in fibroblast cells was investigated in 3 study groups (control cells, UVA untreated cells and treated cells with 200 µg/ml tamarind seed coat extract). The results are shown in Figure 36, 6 h after UVA irradiation, total glutathione of UVA group were significantly increased to 25%, compared to the control, which was set 100%, ( $p < 0.05$ ). This could be implied that one of the cellular responses against UV exposure causing high-level ROS is the regulation of detoxifying enzyme such as glutathione peroxidase. Reduced glutathione has many different functions such as protection against ROS. During the reduction of hydrogen peroxide, Reduced glutathione is converted into an oxidized form, glutathione disulfide (GSSG), and GSSG is reduced back to GSH by NADPH-dependant glutathione reductase (Fang, et al., 2002; Sies, 1999). However, the accumulation of ROS thus reduced the balance of GSH/GSSG resulting in low level of total glutathione as result in 24-72 h of incubation of UVA untreated group.

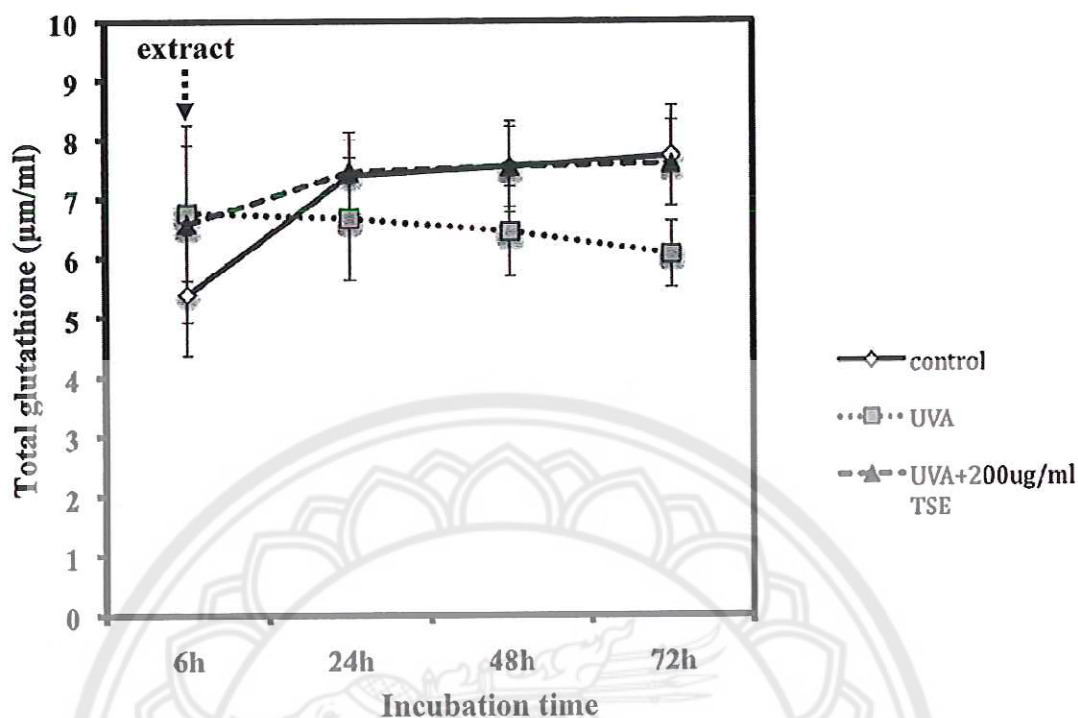


**Figure 36** Effects of tamarind seed coat extract on intracellular GSH/GSSG balance after UVA- induced fibroblasts represent in total glutathione content.

Interestingly, intracellular total glutathione of UVA-induced cells treated with tamarind seed coat extract increased to 10, 20 and 25% compared to the UVA untreated group at 24, 48, 72 h cultivation, respectively (Figure 36, Appendix I). The high total glutathione at 72 h might due to the cell proliferation, correlated to the previous study of cell cycle analysis. The present study demonstrated that tamarind seed coat extract has antioxidant effects by improving the activity of glutathione thus the balance of intracellular GSH/GSSG.

#### 4. Type-I Procollagen and MMP-1 assay

To monitor the biosynthesis and secretion of type-1 collagen and MMP-1, supernatants and cells of subconfluent monolayer cultures were subjected to enzyme immunoassay and immunofluorescence assay. Biosynthesis and secretion were evaluated 6, 24, 48, and 72 h after UVA-irradiation.

At 6 h after irradiation, MMP-1 of UVA irradiated group was found higher than control cells (Appendix J). This indicated the cellular inflammatory responses of fibroblast after UVA exposure. On the contrary, the anti-oxidative effect of the extract against ROS damage might occur causing in low MMP-1 secretion than the ability of immunoassay detection. Nevertheless, a great induction of synthesis and secretion of MMP-1 was found in UVA-irradiated untreated cells as showed in Figure 37. Eighteen hours following treatment by the extract the MMP-1 level significantly decreased to 89% compared to the UVA group ( $p < 0.01$ ), which was set 100%, 48 and 72 h of cultivation the secreted MMP-1 protein decreased to 91 and 56%, respectively. On the other hand, all trans retinoic acid (vitamin A), a well-known MMP-1 inhibitor (Liu, et al., 2009; Frankenburger, et al., 2001) that was use as reference was not effective in our study. The highest MMP-1 content was found when treated with 50 nm/ml vitamin A. This may cause from the variation of cell response to vitamin A as reported previously (Varani, 2000)

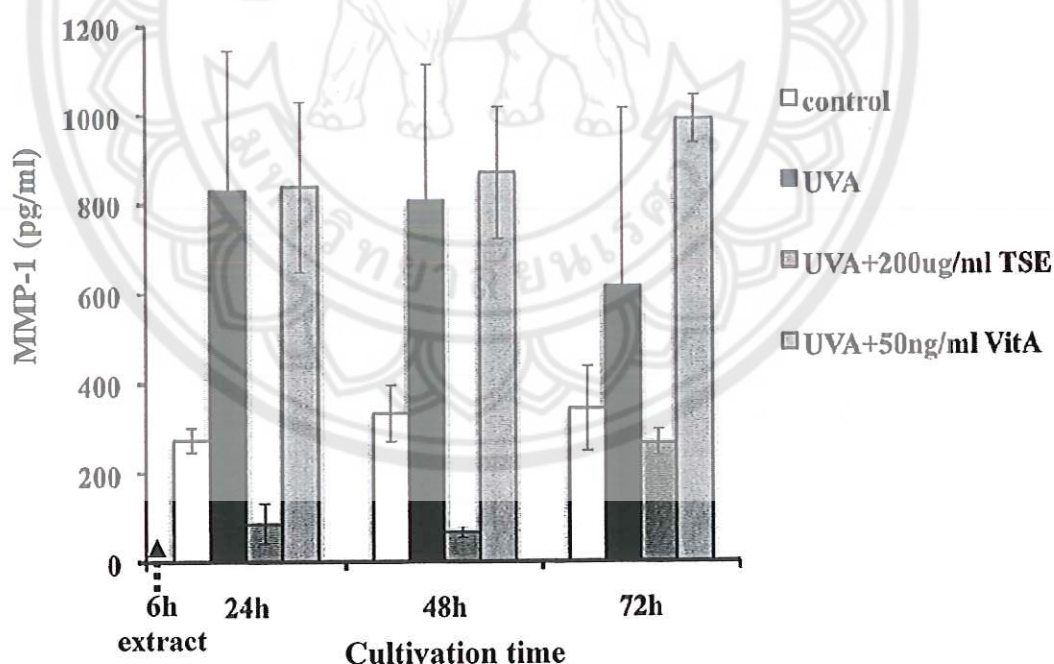


**Figure 37** Effects of tamarind seed coat extract on MMP-1 inhibition in UVA-induced fibroblasts



To confirm the results of enzyme immunoassay, the immunofluorescence assay was performed to detect the location and relative abundance of MMP-1 in fibroblast cells. The fluorescence images of fluorescein (FITC) conjugated with intracellular MMP-1 antibody emitted green color at 520 nm and nucleus staining with DAPI emitted blue color at 461 nm are shown in Figure 38. The results clearly indicated higher MMP-1 content in UVA-irradiated untreated group (Figure 38A) than tamarind seed coat extract treated group (Figure 38C), while the contents of cell nucleus were the same (Figure 38B, D), which indicated that less MMP-1 content of extract treatment was not from cell death.



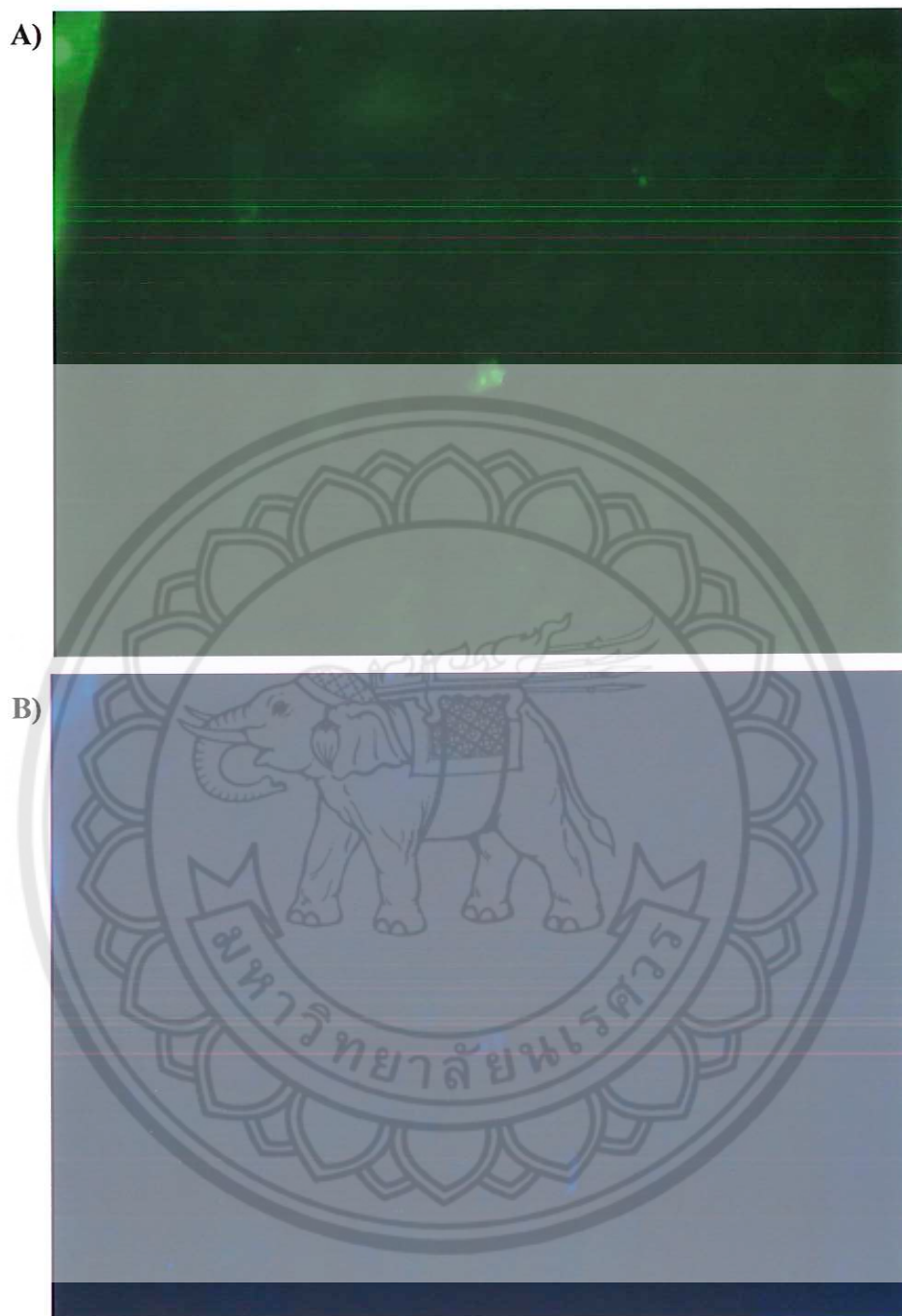


**Figure 38** Fluorescence images of UVA-irradiated untreated group (A-B) and tamarind seed coat extract treated group (C-D). FITC green color indicates MMP-1 content, DAPI blue color indicates fibroblast cell nucleus visualized by fluorescence microscope at magnification of 20X

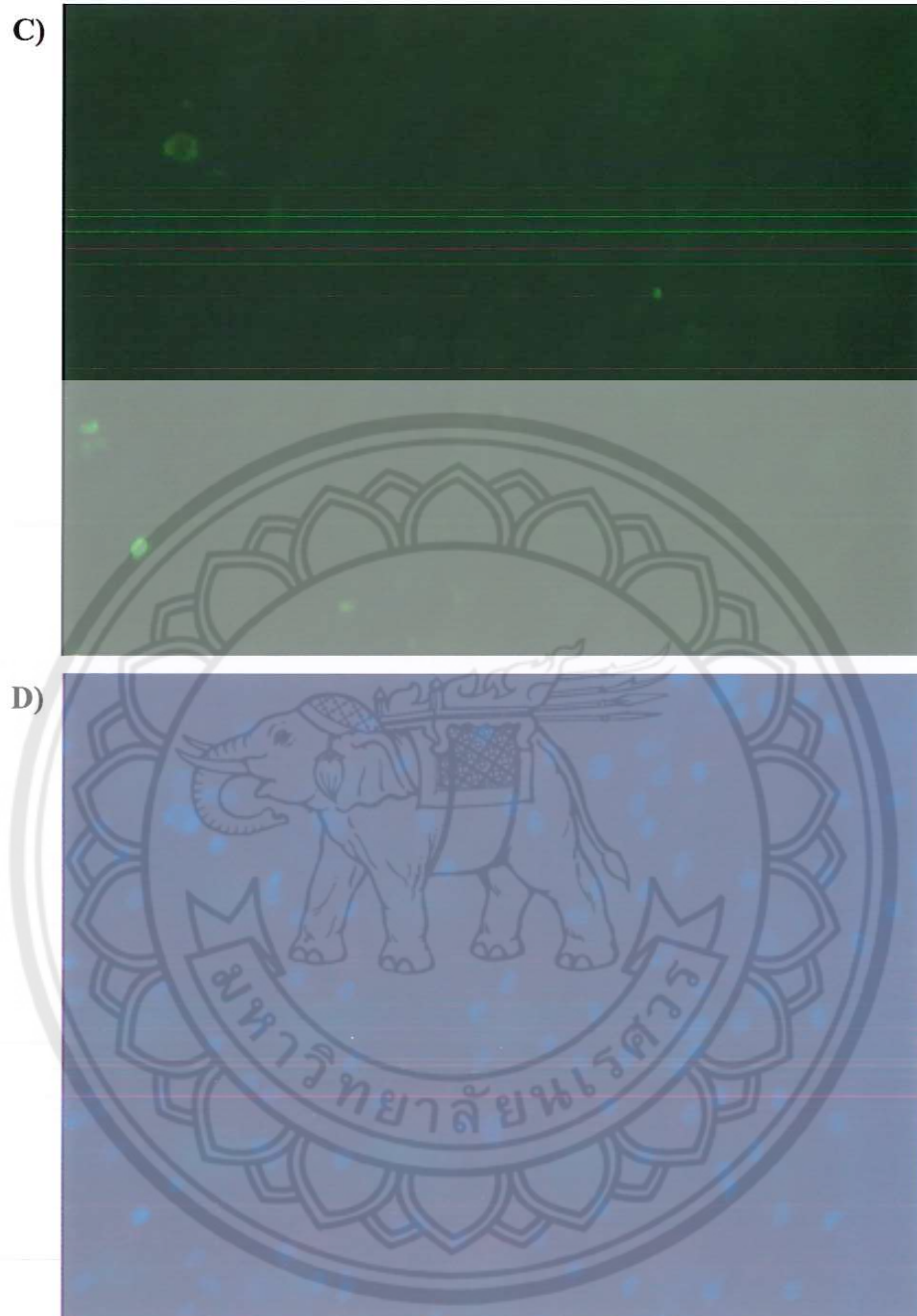
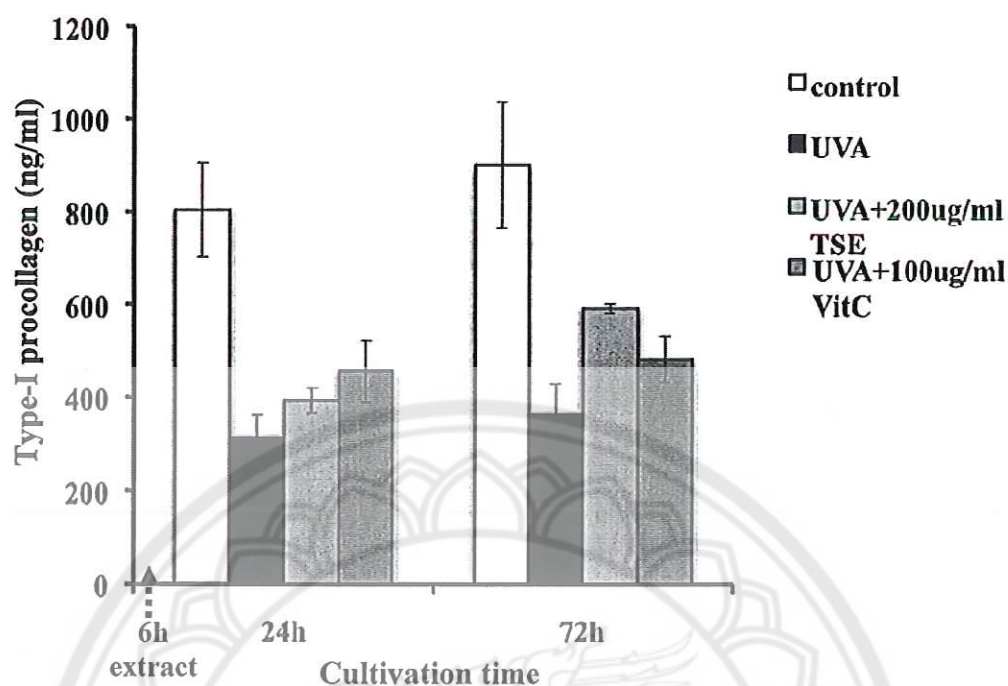


Figure 38 (Cont.)



Taken into consideration, the detection of type-I procollagen synthesis after UVA-induced fibroblast in untreated and treated group was present. At 6 h after irradiation, type-I procollagen continues to secrete extracellular (Appendix J). This indicated the synthesis S phase of cell cycle. As expected, type-I procollagen in control group (non-irradiated) was significantly higher than UVA-treated groups ( $p < 0.01$ ). The results in Figure 39 shown that UVA induced cellular damage caused the 60% decreased type-I procollagen synthesis in fibroblast, comparison to the UVA un-irradiated group ( $p < 0.01$ ), which was set 100%. Interestingly, 18 h following treatment by the extract type-I procollagen significantly increased to 25% compared to UVA irradiated group ( $p < 0.05$ ) and 72 treatment of cultivation the secreted type-I procollagen increased to 63%. On the other hand, L-ascobic acid (vitamin C), a well-known collagen promoter that was use as positive control had more efficacies (16%) promoted synthesis of type-I procollagen than tamarind seed coat extract at first 24 h of cultivation. Besides, tamarind seed coat extract showed the potent efficacy on promoted type-I procollagen synthesis 22% more than vitamin C ( $p < 0.05$ ) after 72 h cultivation. This evidence might indicate the higher stability of tamarind seed coat extract than vitamin C.



**Figure 39 Effects of tamarind seed coat extract on type-I procollagen production in UVA- induced fibroblasts**

The fluorescence images of Cyanine Dyes (Cy5) conjugated with type-I procollagen antibody emitted red color at 670 nm and nucleus staining with DAPI emitted blue color at 461 nm are shown in Figure 40. The low intensity of red color in Figure 40 (A, C) indicated that, type-I procollagen normally secreted extracellular and not remained intracellular. The detection of newly synthesis of type-I procollagen was only exhibit in cell supernatant. However, DAPI stained identified the fibroblast nucleus both in UVA untreated and treated group (Figure 40 B, D).

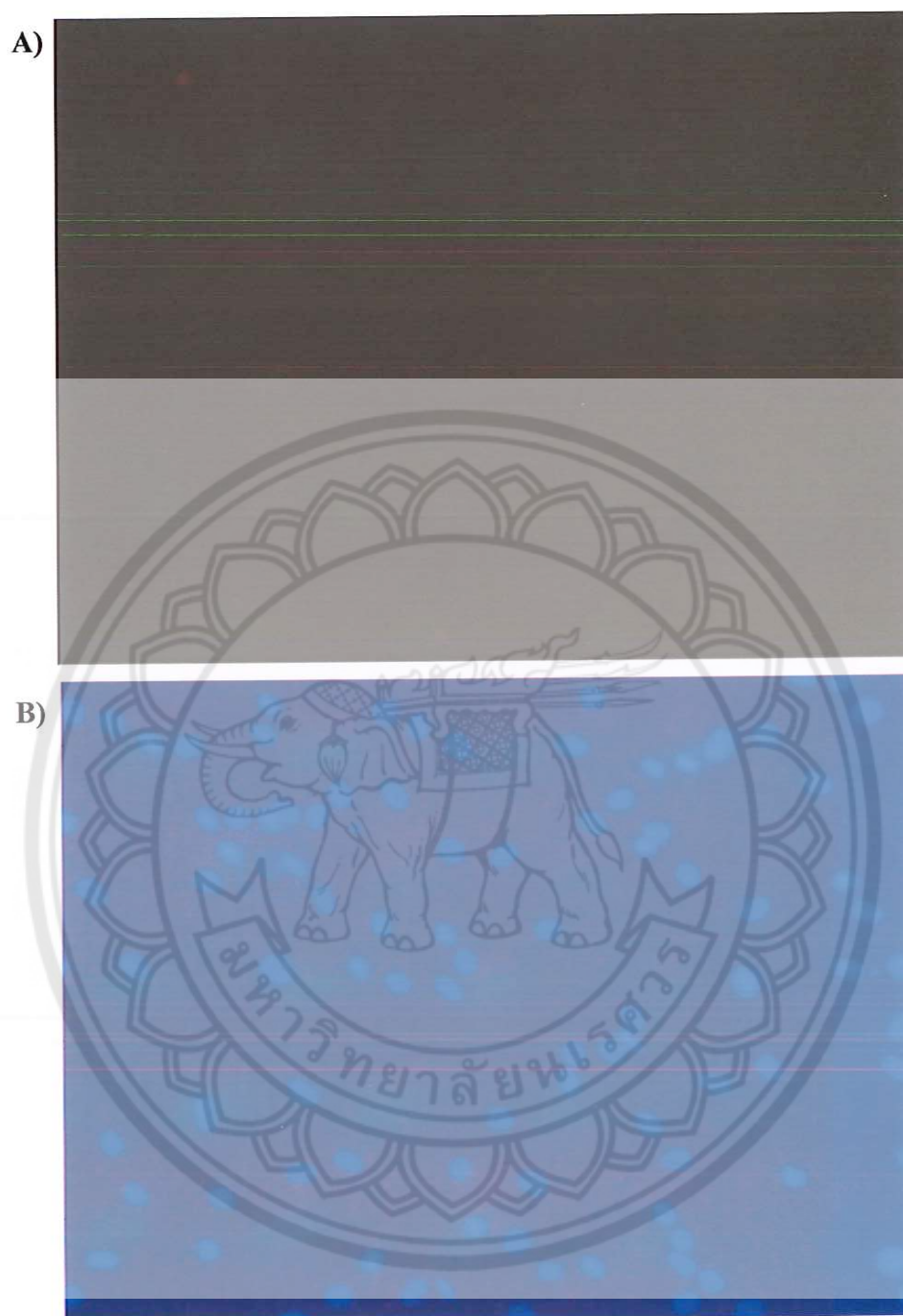


**Figure 40** Fluorescence images of UVA-irradiated untreated group (A-B) and tamarind seed coat extract treated group (C-D). Cy5 red color indicates type-1 procollagen content, DAPI blue color indicates fibroblast cell nucleus visualized by fluorescence microscope at magnification of 20X



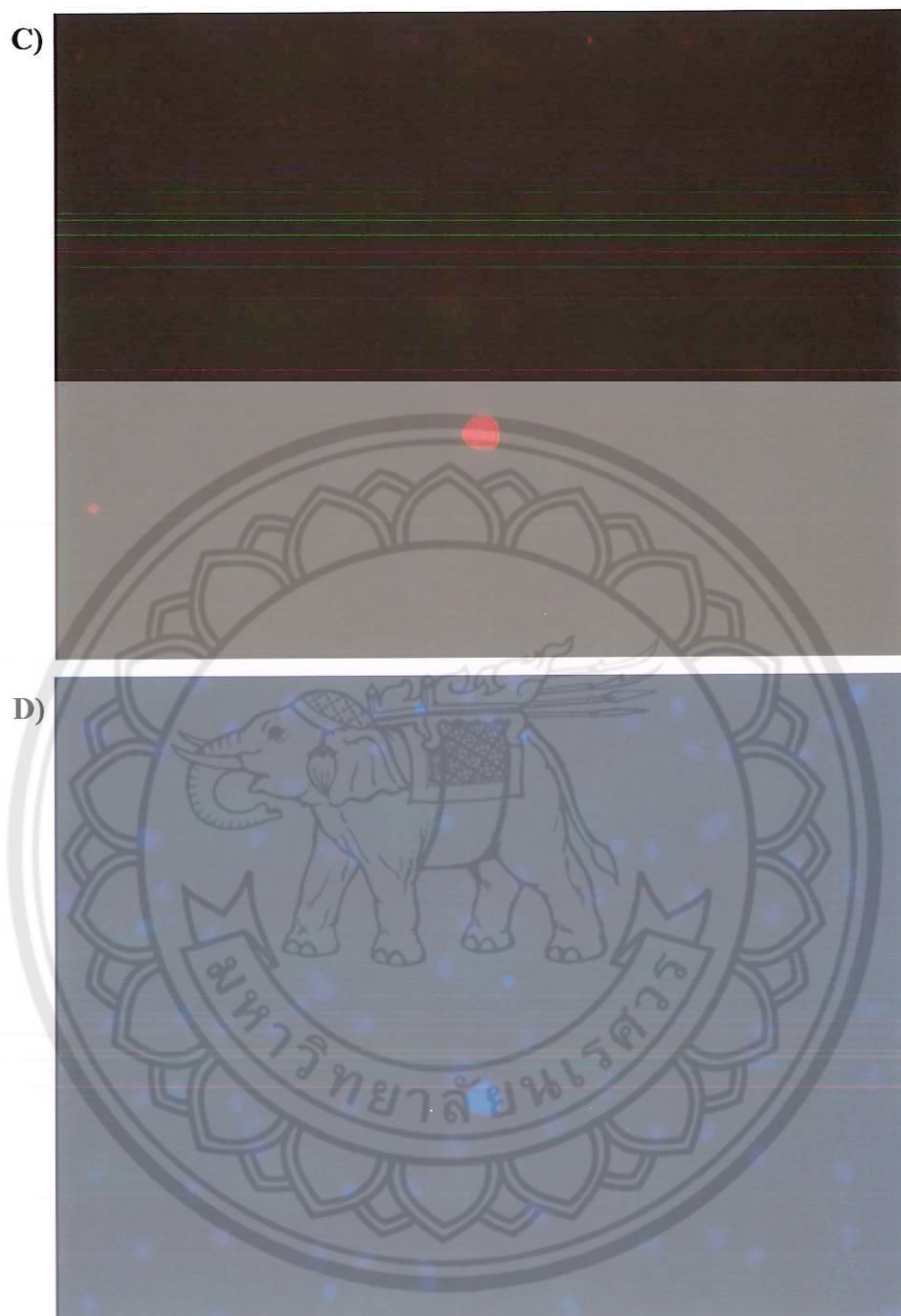


Figure 40 (Cont.)

Photo-oxidative damage caused by solar UV light is the leading cause of extrinsic aging of the skin. Photoaging causes numerous histologic, physiologic, and clinical changes (Kligman, 1986). Acute exposure of solar UV irradiation on the skin induces oxidative stress (Katiyar and Mukhtar, 2001), and oxidative stress is considered to be a major contributor to the process of photoaging of the skin (Harman, 2001; Rittie and Fisher, 2002). Although cellular defense mechanisms including the antioxidant enzymes glutathione peroxidase, glutathione reductase, superoxide dismutase, and catalase have evolved to quench ROS, these antioxidant defense enzymes are not fully efficient, and cells accumulate molecular evidence of oxidative damage. Several studies have shown that there is an age-associated increase in both ROS generation (Sohal and Brunk, 1992) and the level of oxidatively damaged proteins (Stadtman and Levine, 2000). Therefore new chemopreventive agents and strategies need to be developed that can prevent solar UV light-induced oxidative damage, and oxidative damage mediated photoaging process. One of the approaches that have generated enormous interest is the use of antioxidants (Fisher, et al., 1999; Sander, et al., 2002). On photodamaged skin, it has been reported that vitamin A, E, C, and procyanidins exhibit photoprotective effects on skin due to their antioxidant activities (Eberlein-Konig, et al., 1998; Stahl, et al., 2000; Mittal, et al., 2003).

In this study, we found that tamarind seed coat extract inhibited the cell damage that occurred in the fibroblast after acute UVA exposure. Moreover, the reduction of cell cycle arrest in S and G2/M phase and progression of G0/G1 phase also exhibit with tamarind seed coat extract treatment. Most cellular signaling pathways involved in photoaging are mediated through oxidative stress (Katiyar and Elmets, 2001; Rittie and Fisher, 2002). It has been shown that depletion of antioxidant enzymes level in photodamaged skin also associated with higher levels of protein oxidation (Sander, et al., 2002). We also found that fibroblast treated with tamarind seed coat extract resulted in prevention of UVA-induced depletion of antioxidant enzymes such as glutathione peroxidase and the level of glutathione.

Photoaging is characterized by degradation of collagen and accumulation of abnormal elastin in the superficial dermis, several matrix MMPs have been implicated in this process (Saarialho-Kere, et al., 1999; Fisher, et al., 2002; Inomata, et al., 2003). MMP-1, derived from dermal fibroblasts could be ultimately initiated degradation of collagen types I and III. Our study in this photoaging model demonstrates that acute exposure of skin fibroblast to UVA-induced expression of MMP-1, which has been shown to be involved in the degradation of types-I (Rittie and Fisher, 2002). Treatment of tamarind seed coat extract has been shown to reduce UVA-induced MMP-1 and protected fibroblast from the decrease of dermal collagen in fibroblast.

#### **Effect of tamarind seed coat extract on contraction of fibroblast-embedded collagen lattice**

Here, the skin aging improvement of tamarind seed coat extract could be clearly represented in this study. Fibroblast embedded collagen lattice was developed to determined the locomotion and attachment of fibroblasts which related to the collagen metabolism, reorganization and reorientation of collagen fibers that necessary to minimize the development of skin wrinkles (Rakic, et al., 2000; Tamariz and Grinnell, 2002). When fibroblasts interact with collagen matrices, unlike planar surfaces, the cells can penetrate into the substance of the matrix and become entangled with matrix fibrils (Jiang and Grinnell, 2005). Cells interacting with collagen matrices exhibit distinct patterns of signaling and migration (Wozniak, et al., 2004; Evan-Ram and Yamada, 2005) and remodel matrices achieve tensional homeostasis (Tranquilo, 1999) While cells on planar surfaces can modulate their cytoskeletal function in response to surface mechanics (Giannone and Sheetz, 2006).



In this study, the model mimicking the skin-aging pattern was the using of young and old (wrinkled) fibroblasts. Different aged of fibroblasts was growth freely in collagen matrices. The most influence factor to develop collagen lattice was system pH that should not more than 7.4. Moreover, the concentration of collagen was effected the migration of fibroblast, high concentration made lattice too rigid and fibroblast could not freely action. Figure 41 shows fibroblasts interact with collagens in matrices visualized under 20X microscope.

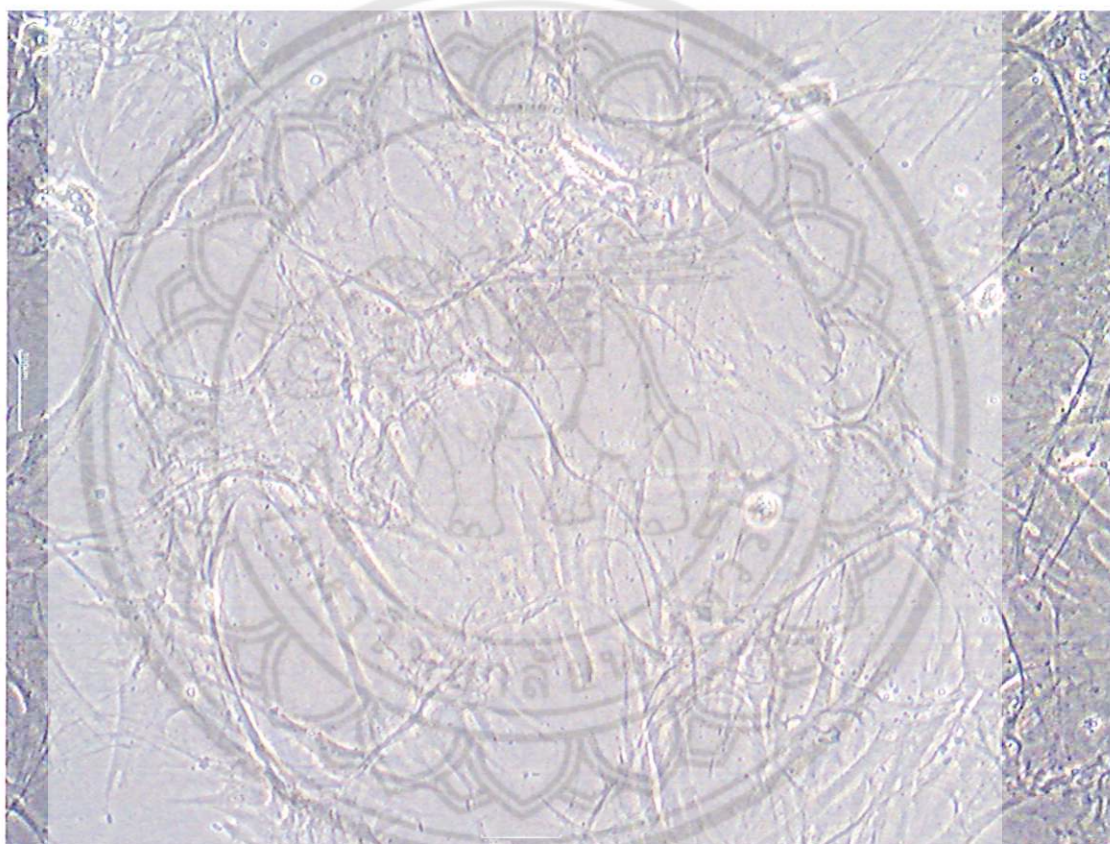


**Figure 41 Micrograph of fibroblast interact with collagen in matrices visualized under 20X microscope at day 2**

Comparison between young and old (wrinkled) skin fibroblast in 3 dimensional collagen lattice, Figure 42 shows the clearly different in lattice diameter, which indicated the fibroblast contraction force within day 5.

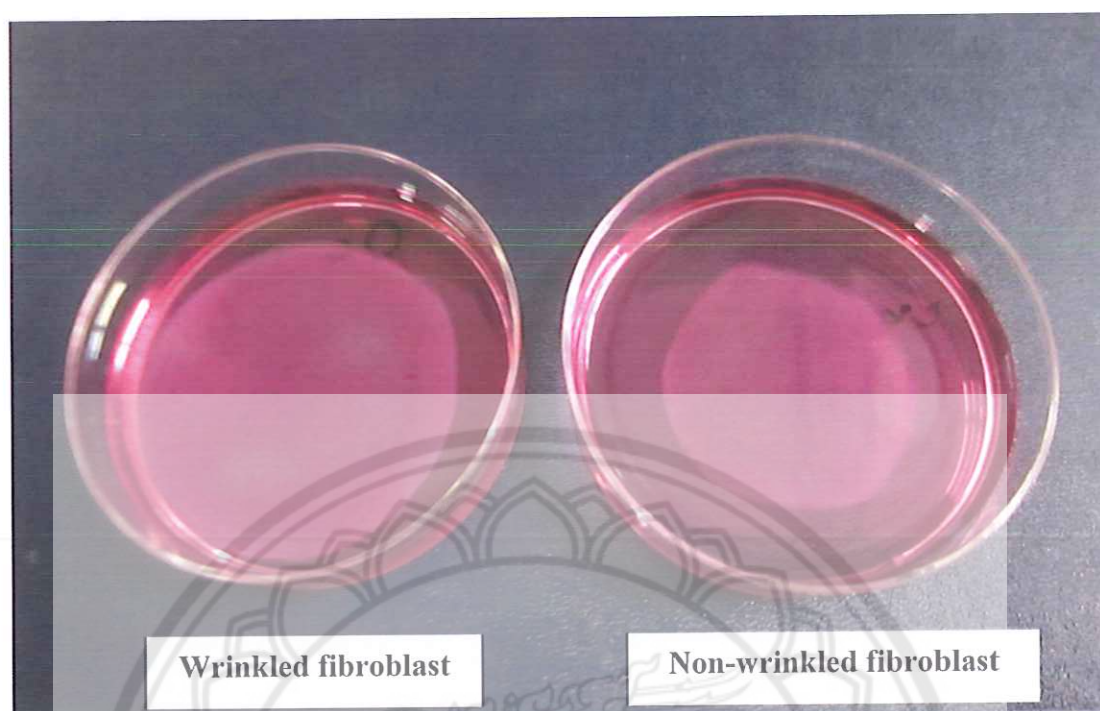


**Figure 42** Photograph of wrinkle and young skin fibroblast embedded with collagen lattices floating singly in the culture dishes at day 5

Normally, young fibroblast has the potential to reorganize and reorientation itself. Surprisingly, the treatment of tamarind seed coat extract showed the extent of contraction (initial diameter decreased by 41%) of lattices populated with young (nonwrinkled-skin) fibroblasts vigorously for the first 3 days compared to control with the significantly different ( $p < 0.05$ ) (Figure 43, Appendix K). While the diameter decreased by 60% appeared at day 5 and the highest contractions up to 70% of initial diameter occurred by the treatment of tamarind seed coat extract, which was 2-fold higher than control.



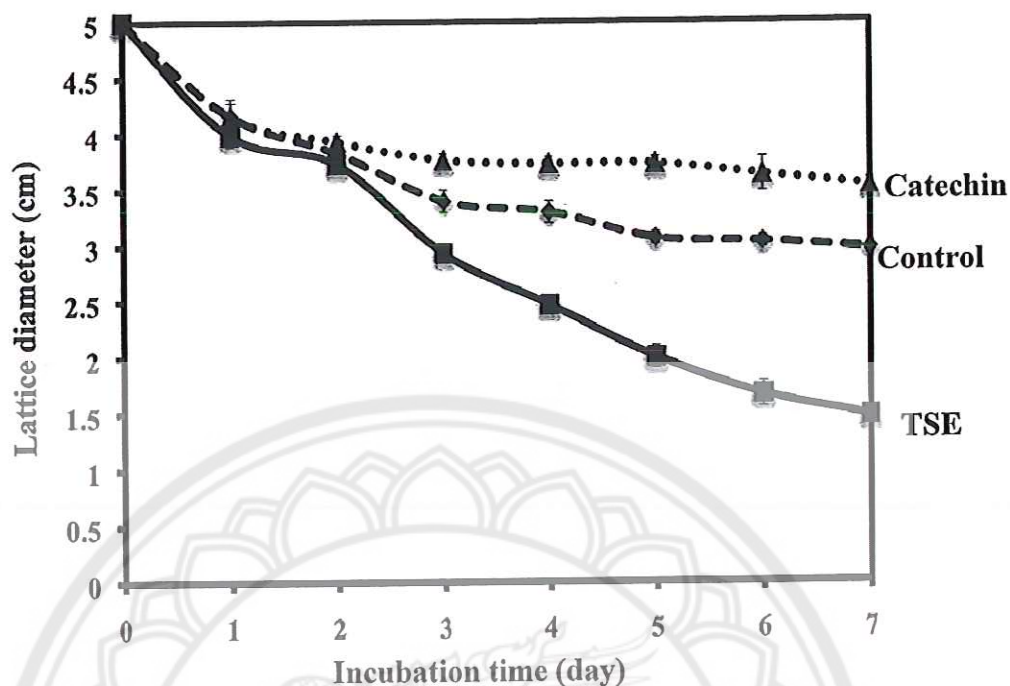


**Figure 43** Effect of tamarind seed coat extract (TSE) on contractile capacity of nonwrinkled-skin (young) fibroblasts. Fibroblasts embedded in the collagen lattice were treated with DMEM (control) or 200  $\mu\text{g}/\text{ml}$  extract or 20  $\mu\text{g}/\text{ml}$  catechin. The diameter of each lattice was measured over 7 days of culture. Each point represents mean  $\pm$  S.D. of three samples in duplicate

The effects of tamarind seed coat extract on promoting the reorganization of fibroblast could be clearly visualize in Figure 44. The lattices, which slightly not round shape, might occur from the high-tension force of fibroblast. The rapid contraction began at day 3 and constant at day 7.



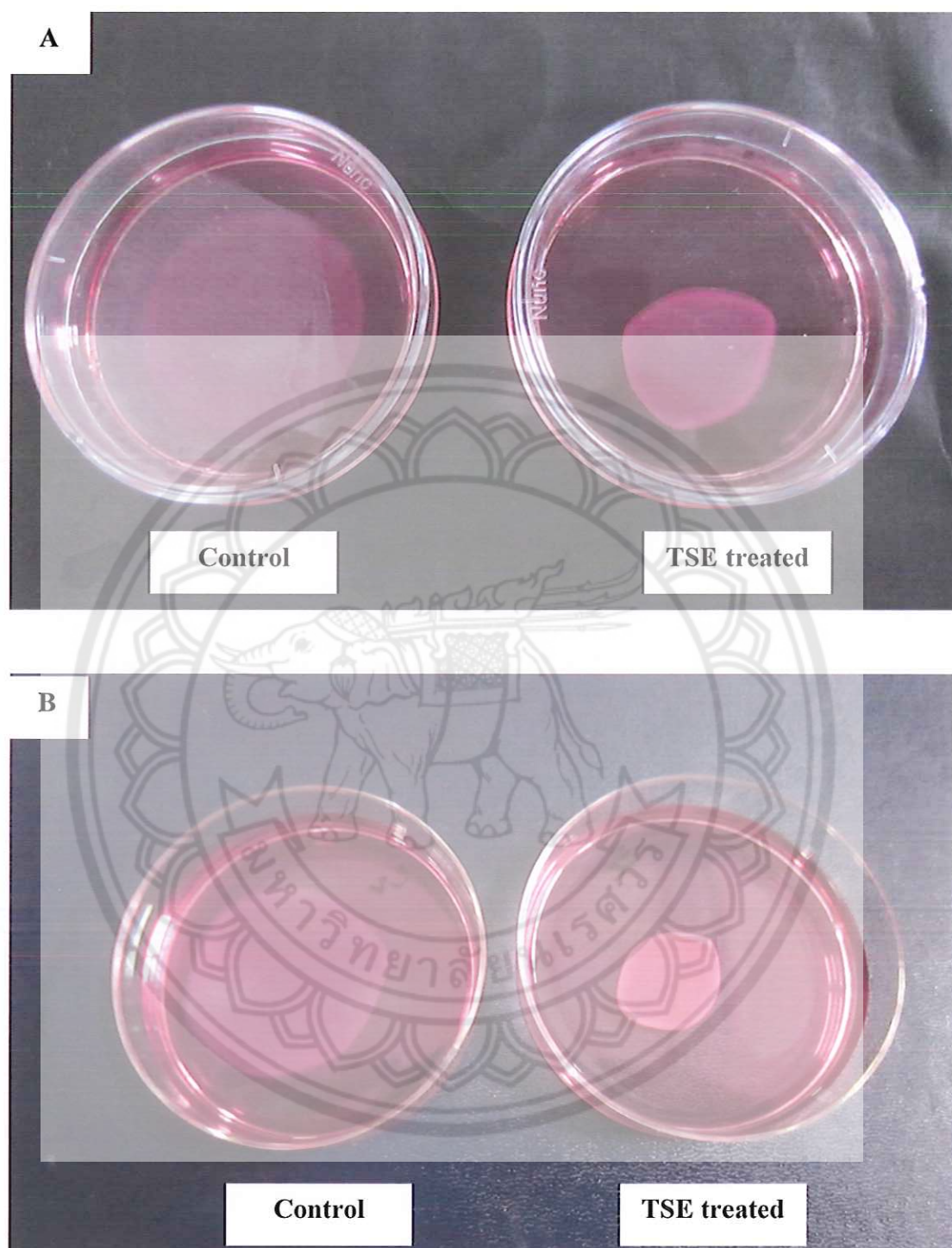


**Figure 44** Photographs of non-wrinkled skin fibroblast embedded with collagen lattices treated with DMEM (control) or 200 µg/ml extract (TSE), floating singly in the culture dishes at day 5 (A), and day 7 (B)

On skin aging simulation, wrinkled fibroblasts were embedded in collagen matrices. Notwithstanding, tamarind seed coat also showed the efficacious in promoting fibroblast reorganization. The results from calculated the lattice diameters are shown in Figure 45. The treatment of tamarind seed coat extract showed the extent of contraction (initial diameter decreased by 33%) of lattices populated with wrinkled fibroblasts vigorously for the first 3 days compared to control (Figure 45, Appendix N). The significantly different ( $p < 0.05$ ) occurred at day 4, while the diameter decreased by 42%. The highest contractions up to 53% of initial diameter occurred by the treatment of tamarind seed coat extract.

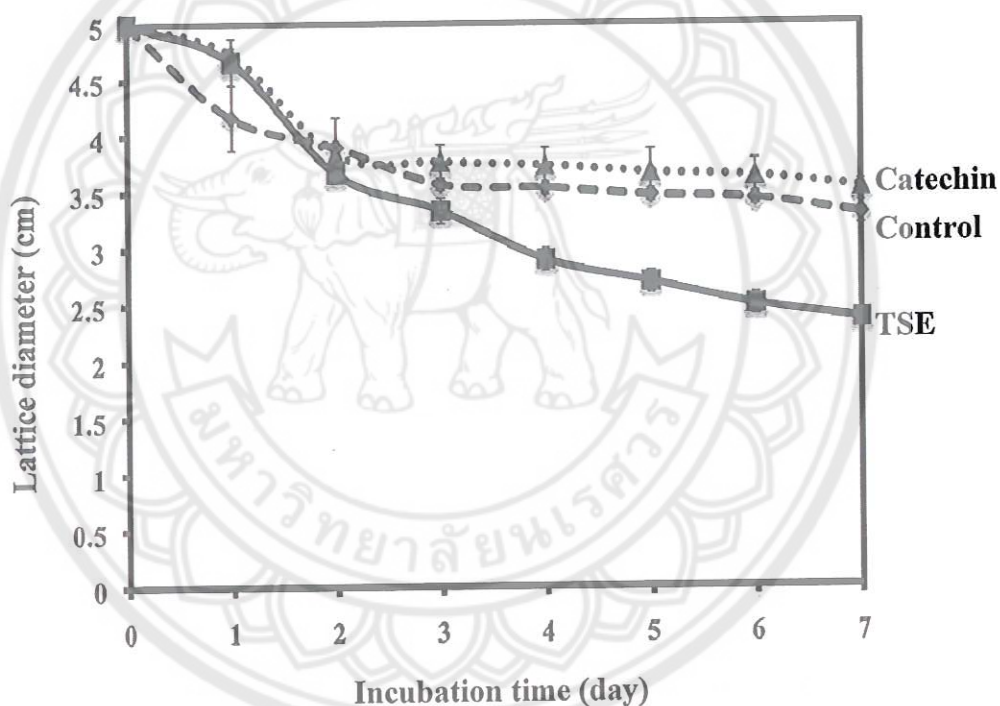


**Figure 45** Effect of tamarind seed coat extract (TSE) on contractile capacity of wrinkled skin fibroblasts. Fibroblasts embedded in the collagen lattice were treated with DMEM (control) or 200  $\mu\text{g/ml}$  extract or 20  $\mu\text{g/ml}$  catechin. The diameter of each lattice was measured over 7 days of culture. Each point represents mean  $\pm$  S.D. of three samples in duplicate.



Figure 46 showed the clearly effects of tamarind seed coat extract on promoting the reorganization of wrinkled fibroblast. Unlike young fibroblast, less tension force of fibroblast cause slowly contracted.

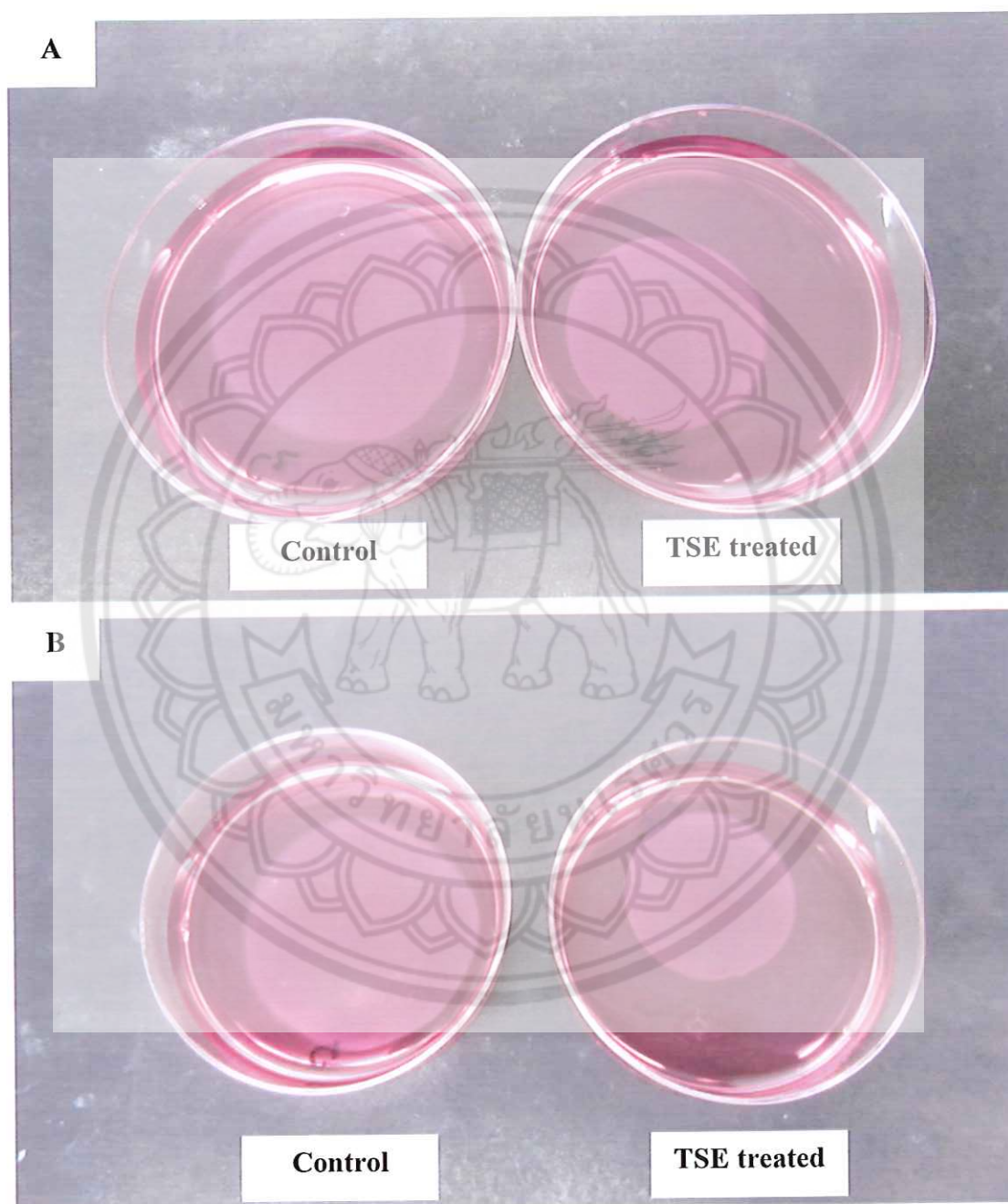


**Figure 46** Photographs of wrinkled skin fibroblast embedded with collagen lattices treated with DMEM (control) or 200 µg/ml extract (TSE), floating singly in the culture dishes at day 5 (A), and day 7 (B).



On the contrary, the effect of standard catechin (one of the main phenolic compound in tamarind seed coat) was unpredictable. After treated with catechin, fibroblasts tended to lose their ability to reorganized and function. At day 7, the contractile of catechin-treated collagen lattice (initial diameter decreased by 29% both in young and wrinkled fibroblast groups) even less than control (initial diameter decreased by 34% and 40% in young and wrinkled fibroblasts, respectively). The photograph showed comparisons between 3 groups in Figure 47. It is possible that catechin at used dose could enhance the cellular oxidative damage and isolated DNA through the generation of reactive oxygen species (Oikawa, et al., 2003; Rathore, et al., 2012) This could be implied that the usage of natural crude extract should have more benefit effect than pure compound as the present of other compounds might minimize the activity of toxic compounds

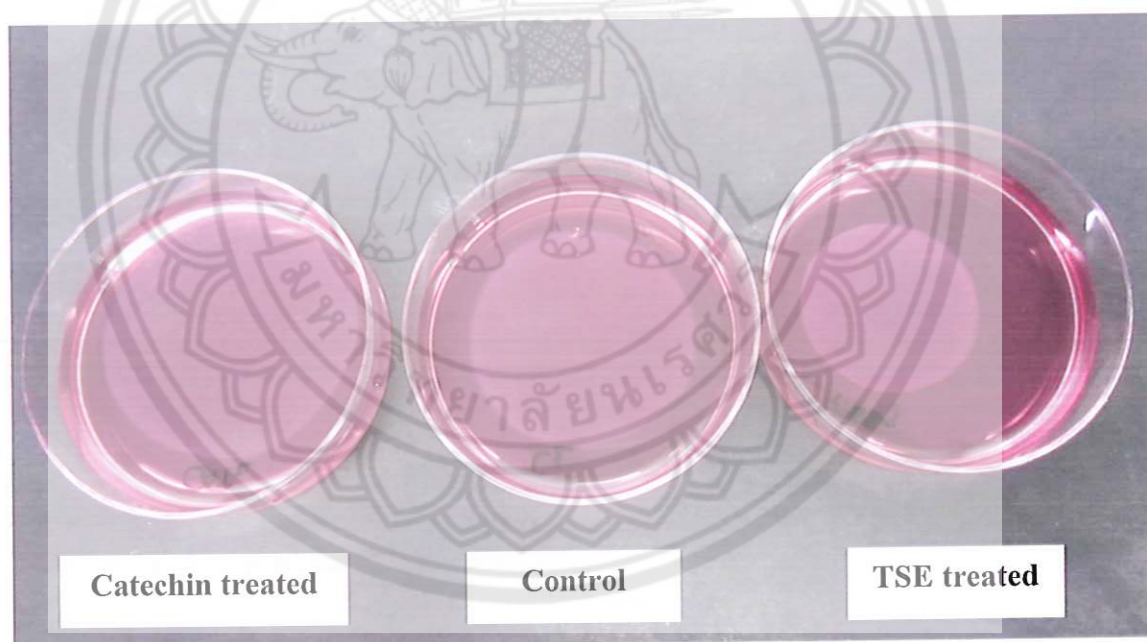


**Figure 47 Photographs of wrinkled skin fibroblast embedded with collagen lattices treated with DMEM (control) or 200  $\mu\text{g/ml}$  extract (TSE) or 20  $\mu\text{g/ml}$  catechin, floating singly in the culture dishes at day 7**

In attempting to identify biochemical markers of contraction, consideration must be given to the cellular activity underlying it. The theory that has received the most research emphasis to date is that contraction occurs secondary to the differentiation of fibroblasts to form active myofibroblasts with expression of alpha-actin filament bundles (Gabbiani and Majno, 1972; Tomasek and Haaksma, 1991; Welch, 1992). These myofibroblasts possess intrinsic contractile properties similar to smooth muscle cells and organise their actin cytoskeleton along the lines of greatest skin tension (Petrol, et al., 1993). The actin filaments become more compact due to a sliding-filament mechanism involving actin and myosin filaments. The majority of studies of fibroblast and myofibroblast behaviour in contraction have been carried out using fibroblast-embedded collagen lattice. These three-dimensional lattices induce morphological changes in fibroblasts that at least partially mimic those seen in vivo (Elsdale and Bard, 1972).

In skin aging, the study of dermal rather than epidermal or total thickness appears to be the important factor. These studies show without doubt that tamarind seed coat extract are capable of exerting considerable on fibroblast embedded collagen lattice by promoting myofibroblast activity, thus maintaining function of active fibroblast.